The Transient Localization Scenario for Charge Transport in Crystalline Organic Materials

Simone Fratini, D. Mayou, S Ciuchi

The Transient Localization Scenario for Charge Transport in Crystalline Organic Materials.

S. Fratini*, D. Mayou, and S. Ciuchi

August 26, 2015

Abstract

Charge transport in crystalline organic semiconductors is intrinsically limited by the presence of large thermal molecular motions, which are a direct consequence of the weak van der Waals inter-molecular interactions. These lead to an original regime of transport called *transient localization*, sharing features of both localized and itinerant electron systems. After a brief review of experimental observations that pose a challenge to the theory, we concentrate on a commonly studied model which describes the interaction of the charge carriers with inter-molecular vibrations. We present different theoretical approaches that have been applied to the problem in the past, and then turn to more modern approaches that are able to capture the key microscopic phenomenon at the origin of the puzzling experimental observations, i.e. the quantum localization of the electronic wavefuntion at timescales shorter than the typical molecular motions. We describe in particular a relaxation time approximation which clarifies how the transient localization due to dynamical molecular motions relates to the Anderson localization realized for static disorder, and allows us to devise strategies to improve the mobility of actual compounds. The relevance of the transient localization scenario to other classes of systems is briefly discussed.

[*] Dr. S. Fratini, Dr. D. Mayou
Institut Néel, CNRS and Université Grenoble Alpes, F-38042 Grenoble, France
E-mail: simone.fratini@neel.cnrs.fr

Prof. S. Ciuchi
University of L'Aquila, Department of Physical and Chemical Sciences, Via Vetoio, L'Aquila, Italy; CNR-ISC, Via dei Taurini, Rome, Italy; CNISM, Udr L'Aquila, Italy

Contents

1 Introduction

Molecular organic semiconductors, i.e. solids composed of small organic molecules, have gained a rising interest in the past years because of their implementation as active semiconductor layers in electronic and opto-electronic devices. These range from field-effect transistors to lightning devices and displays, photovoltaic cells and novel spintronic devices. In parallel with such applied developments, remarkable advances have been made in understanding the electronic properties of organic semiconductors, triggered by the great improvements in sample and device fabrication. While in the past, the physical properties in these compounds were often masked by impurity effects or structural inhomogeneities, it has now become possible to investigate high-quality crystals via a broad panel of experimental techniques, giving access

to the intrinsic properties of the electronic charge carriers and their correlation with the microscopic material parameters.

The quantity which has concentrated most efforts of both applied and fundamental studies is the charge carrier mobility μ. This is a key material parameter because it influences the performances of actual semiconductor devices, such as the switching rate in transistors or the efficiency of energy transfer processes in photovoltaics. [1, 2] At present, mobilities in excess of $10cm^2/Vs$ can be achieved in organic field-effect transistors (OFETs) based on crystalline organic solids, [3] and comparable values are also observed in OFETs with ordered films. [4] Such values are much higher than those characterizing amorphous organic films ($10^{-4} - 10^{-5}cm^2/Vs$) but remain orders of magnitude lower than those found in wide-band semiconductors, reaching values higher than 10^7 in inorganic semiconductor heterostructures, 10^6 in graphene, 10^3 in crystalline silicon and several 10^2 in transition-metal dichalcogenides.

This intrinsically low mobility indicates extremely short electronic mean-free paths — on the order of the intermolecular distances — leading to a breakdown of the basic assumptions underlying band transport theory. It is currently believed that the mobility in crystalline organic semiconductors, at least within the technologically relevant regime around room temperature, is intrinsically limited by the presence of large thermal molecular motions, which are a direct consequence of the weak van der Waals intermolecular interactions. Deviations from the perfect crystalline arrangement, and thus from a periodic Bloch-state, act as a dynamical source of disorder on the already narrow electronic bands arising from the π-intermolecular overlaps. These induce a localization of the electronic wavefunctions, which survives up to the typical time scales of the inter-molecular vibrations. This phenomenon, that is not described by the semi-classical Boltzmann theory of electron-phonon scattering, results in an original transport mechanism that was termed *transient localization*. It is our purpose here to review the recent theoretical advances and experimental successes of the transient localization scenario for charge transport in crystalline organic solids.

Organic semiconductors: between the solid state and molecular pictures. – The order-of-magnitudes difference in the mobility of even the best organic semiconductors as compared to their wide-band counterparts testifies that charge transport in these materials is not governed by the same microscopic mechanisms. In the early days of organic semiconductor research more than 50 years ago, several alternative approaches were proposed. Attempts to describe organic semiconductors were made either extending the realm of semi-classical Boltzmann theory beyond the standard treatments which apply to inorganic semiconductors, or using radically different theoretical concepts to start with, such as Marcus theory and Holstein small polaron theory, i.e. focusing on the molecular rather than the "band" character of these compounds. [5] However, none of these has provided a truly satisfactory and consistent description of the charge dynamics. In the years following these early works, researchers concentrated their efforts in extending such original concepts and including more realistic material details, determining the microscopic parameters from *ab initio* methods with ever increasing accuracy, which was made possible by the great improvements in the numerical calculation capabilities. It is however fair to say that no real theoretical breakthrough emerged from these studies: the well-known Marcus formula for hopping transport, for instance, still remains widely used today to evaluate the mobility in fully *ab initio* treatments of specific compounds, even though its very assumptions are violated in high-mobility organic semiconductors.

From a theoretical point of view, the difficulty in addressing charge transport in organic materials comes from the fact that several microscopic interactions are at work, whose characteristic energy scales are all of comparable magnitude, thus preventing the applicability of standard limiting treatments. The typical values of the intermolecular transfer integrals, which determine the bandwidth of extended electronic states moving through the solid, are in the range $J \sim 10 - 100meV$. This is comparable to the energy gained upon deformation of the individual molecules to accommodate excess charge carriers (i.e. the polaron energy or relaxation energy), $E_P \sim 50-200meV$, [6, 7, 8, 9] which instead favors localization of the carriers on individual molecules. This "intermediate coupling" situation prevents in principle the use of both Marcus theory, which is only applicable when the intermolecular transfer energy J is the smallest energy scale in the problem, and standard band theory, which instead requires it to be the largest: neither of these limits is fulfilled organic semiconductors materials. Another important parameter which influences the carrier dynamics is the zero-point energy of molecular vibrations. In the case of the intra-molecular modes, these also lie in the range $\hbar\Omega_0 \simeq 100 - 200meV$. The carriers also interact with lower energy inter-molecular modes, in the range $\hbar\omega_0 \lesssim 10meV$. [9, 10, 11] Finally, the thermal energy $k_BT \sim 25meV$ at the ambient conditions relevant for technological applications is also of the same order of magnitude.

The absence of an identified small parameter makes it difficult to find a proper starting point on which to apply perturbation expansions, which is often at the origin of long-standing and unsolved problems in physics. In this respect, organic charge transport is no exception to the rule.

The emergence of an alternative paradigm. – In this theoretical no man's land, an alternative scenario that was proposed early on to describe charge transport in organic semiconductors (see Ref. [5] for an early re-

view) has been gaining strong support in the last decade. It starts from the observation that, because the inter-molecular Van der Waals forces which hold organic solids together are weak, thermal molecular motions in these materials can be very large. Such motions are slow due to both the weak restoring forces and the large molecular masses, and provide the electrons at each instant of time with a very disordered landscape that is strongly detrimental to their mobility. In this view, the presence of such unavoidable disordered molecular landscape constitutes the main and ultimate limiting factor of the mobility in organic semiconductors.

The above observation calls for a change of paradigm from the conventional view of charge carriers being weakly scattered by phonons, to one where charge carrier motion is hindered by a slowly varying, strongly disordered environment. [1] Accordingly, one should observe even in the best organic semiconductors some of the characteristic features of localization in disordered systems, and indeed there have been numerous reports of some form of localization of the carriers' wavefunctions in organic semiconductors (see Sec. 2.1 below). Albeit slow, however, thermal molecular displacements are by nature dynamic. This constitutes a fundamental difference from the static chemical or structural disorder, which instead can cause full localization of the charges via a fully quantum process known as Anderson localization. [12] For this reason, established theories of disordered conductors and semiconductors [12, 13, 14, 15] cannot be directly applied to the problem, no more than the band, Marcus and polaron theories discussed above.

The most striking consequence of dynamical disorder is that contrary to the static case, it does not lead to the occurrence of thermally activated and exponentially suppressed mobilities, which are instead commonly observed in amorphous and disordered semiconductors. [13] Consequently, although a strong thermal molecular disorder is inherently present in high quality organic crystals, the mobility in these systems exhibits a power-law temperature dependence which is reminiscent of semi-classical band-like behavior, in apparent contradiction with the disordered picture. One of the main requirements for the theory is to solve this contradiction, accounting for both the intrinsic localization effects brought in by the strong molecular motions, and the apparent band-like behavior of the mobility.

Transient localization: time for an overview. – The ideas presented above constitute the basis of the *transient localization* scenario for charge transport in organics. Starting from the pioneering works on a paradigmatic microscopic model that captures the essential aspects of the phenomenon, [5, 16, 17, 18, 19] a number of recent theoretical works have analyzed the problem by applying different numerical, analytical and phenomenological approaches. As a result of these recent studies, both a solid theoretical framework and a more transparent physical picture of the charge transport mechanism are now emerging. From the experimental point of view, several key experiments are in agreement with the transient localization scenario, and an increasing number of results is now discussed in terms of these ideas. [20, 21, 22, 23, 24, 25]

Despite a number of review articles and books published on the subject of charge transport in organic semiconductors, this important theoretical framework has not been comprehensively described in any review yet (although some aspects are mentioned in Refs. [21, 26, 27]). Because it is now reaching its full theoretical maturity, and in order to set the ground for more systematic experimental confirmations, we consider that it is now timely to provide an overview of the transient localization scenario.

The present article has no ambition to be exhaustive on the different theories of charge transport in organic semiconductors. For these purposes, we refer the reader to existing reviews on the subject, e.g. [1, 5, 21, 27, 28, 29, 30, 31, 32]. Our aim here is to focus on the simplest and most studied model that captures the essential aspects of charge transport in organic semiconductors: Eq. (1) — which describes the motion of electrons on a one-dimensional molecular stack, linearly coupled to inter-molecular vibrations. We shall present the different theoretical approaches that have been applied to it, and compare the different theories with existing experimental results. For the sake of clarity, whenever possible we shall compare the results of different approaches by keeping one given set of parameters corresponding to rubrene, for which reliable theoretical estimates are available. This will allow us to benchmark the different methods that have been applied to the calculation of the mobility, assessing how they perform on an experimentally relevant example. [2] For the same reasons exposed above, we choose rubrene as a reference experimental material, which is one of the most studied high mobility organic

[1] Inter-molecular vibrations in organic semiconductors are only moderately coupled to the electron motion (inter-molecular electron-phonon coupling constants $E_P \lesssim 10meV$ are roughly one order of magnitude lower than the couplings with intra-molecular modes), but their effect of on transport is strong owing to their large amplitude. This particular regime lies beyond the limits of applicability of available electron-phonon coupling theories, so that an alternative starting point (i.e. viewing them as a slow dynamical disorder) becomes more sensible. In more rigorous terms, what is needed is a theory able to describe a weak or moderate coupling to pre-existent large molecular vibrations of thermal origin, to be contrasted with the well explored polaronic theories which involve a strong coupling with carrier-induced molecular deformations.

[2] Due to the large amount of theoretical results that have been produced in more than half a century of research, it is not an easy task for the unexperienced reader to distinguish which predictions for the mobility result from different microscopic models (say, coupling to intra-molecular vibrations vs. coupling to inter-molecular vibrations), which ones result from a given model but in different parameter regimes (e.g., coupling of electrons to molecular vibrations in the strong coupling regime, $J \ll E_P$, or in the weak coupling regime, $E_P \ll J$), and which ones result when different approximate schemes are applied to the same model and with the same set of microscopic parameters. This article tries to answer the latter, focusing on the specific case of Eq. (1).

semiconductors.

The outline of this article is the following. In Sec. 2 we start by briefly reviewing a number of experimental results that are of direct relevance to the present scenario. We then present the different possible interactions at work in organic semiconductors and build the reference microscopic model that will be considered in the following. In Sec. 3 we give a brief account on how traditional theoretical approaches perform on such model. Sec. 4 describes modern approaches that take quantum localization effects into account, leading to the transient localization scenario for charge transport. The relevance of transient localization to organic conductors and other degenerate systems is also discussed. Sec. 5 provides a brief summary of the results presented in this overview.

2 Experimental background and theoretical modeling

2.1 Experimental overview

We present here some key experimental observations that are puzzling or contradictory from the point of view of the available descriptions of organic semiconductors, calling for a new theory for charge transport.

Charge transport.– The mobility values are low, falling below the Mott-Ioffe-Regel limit (see Sec. 3.1.2). Attempts to extract a mean-free-path from the band parameters yield values comparable to or shorter than the inter-molecular spacing. This is in contradiction with the very assumptions of Bloch-Boltzmann band transport theory. Yet, in sufficiently pure samples and at sufficiently high temperatures where extrinsic disorder effects are not crucial, the temperature dependence of the mobility in the best organic semiconductors appears to follow a power-law, as would be expected in conventional semiconductors.

The Seebeck coefficient reported in Ref. [33] also seems to be consistent with a "band-like" behavior. The observation of a free-electron like Hall resistance [34] indicates that at least part of the carriers' wavefunctions are extended over several molecules, as such delocalization is necessary for the Lorentz force to have an effect on the electron motion. [21]

Photoemission.– Early experiments on the photoemission spectra of organic molecules in the gas phase allowed to assess the presence of a sizable coupling between the molecular orbitals and the intra-molecular vibrations [7], confirming the values of the relaxation energy E_P predicted by theoretical calculations. More recently, systematic angle-resolved photoemission experiments (ARPES) performed in crystalline organic semiconductors have shown beyond any doubt that such a coupling is not sufficient to destroy or even substantially shrink the electronic bands as would be predicted by polaron theory (cf. Sec. 3.2 below). Because well defined dispersive bands do exist in high-mobility organic semiconductors, theories which start from the molecular limit where the inter-molecular integrals J are assumed to be small compared to the other energy scales should be taken with extreme care.

Electron diffraction.– The occurrence of large thermal molecular motions has been predicted to be a crucial factor in limiting charge transport in organic semiconductors (cf. Sec. 4). To address the question experimentally, the structural dynamics of crystalline samples of a pentacene derivative have been investigated via electron diffraction [23]. Signatures of the thermal inter-molecular motion have been identified in the form of streaks in the diffraction patterns, which could be directly related to the presence of large inter-molecular sliding motions. The average spread of dynamical displacements has been estimated to be of the order of $\sim 0.1\mathring{A}$ at room temperature.

Band tails.– A tangible consequence of such large molecular motions is that the electronic energy vs. momentum dispersion is no longer sharply defined. Because the inter-molecular transfer integrals are themselves strongly fluctuating quantities, tails are expected to emerge in the density of states beyond the band edges. Such tails can be addressed experimentally from the analysis of the electrical characteristics of field effect transistors. Recent works in this direction have shown that even when extrinsic sources of disorder are removed, band tails of intrinsic origin remain, with an extension of few tens of meV. Such intrinsic tails have been ascribed to the presence of thermal molecular motions. [35, 36]

Optical conductivity.– Measuring the optical conductivity of charge carriers in organic semiconductors is experimentally challenging, as these must be injected either in a field-effect transistor (FET) geometry (in which case the absorption measurement is complicated by reflections at the interfaces) or by optical pumping (which is in principle free from interface effects but drives the system out of equilibrium). Despite the experimental difficulties, there have been several reports of the optical conductivity of excess carriers in rubrene. Measurements by different groups [37, 38, 24] agree in showing a markedly non-Drude behavior at room temperature: the optical conductivity exhibits a finite frequency maximum in the far infra-red range, indicating a breakdown of semiclassical behavior, which has been ascribed to some form of localization of the charge carriers. [38] We will come back to this crucial observation in Sec. 4, when analyzing the predictions of the transient localization mechanism concerning the carriers' optical response.

Other probes of a finite localization length.– ESR measurements in different materials have pointed to

the existence of a finite extension for the carrier wavefunctions, typically on few molecular units. [39, 40, 41] It is not clear however if the obtained lengths should be associated to the presence of intrinsic thermal disorder or to trapping by extrinsic sources of disorder. In any case, these findings provide strong indications that a true quantum localization process takes place in organic semiconductors. The optical charge modulated spectroscopy (CMS) measurements of Ref. [4, 22] in pentacene derivatives are also compatible with the existence of a finite localization length, coexisting with a band-like power-law dependence of the mobility.

2.2 Microscopic mechanisms at work

Several microscopic mechanisms have been considered in order to explain the low electronic mobilities in molecular organic semiconductors. These include the coupling of electrons to low-frequency, inter-molecular vibrations; the coupling of electrons to high-frequency, intramolecular vibrations; the coupling to fast electronic polarization modes; the presence of bulk static disorder, of both chemical and structural origin as well as interface disorder and polarization, when the material is placed in a FET geometry. Although all these phenomena can certainly play a role, we shall focus in this article solely on the coupling to slow inter-molecular modes, which is now emerging as the main intrinsic mechanism limiting charge transport in the best organic semiconductors. Before moving on to the detailed model description of this phenomenon in Sec. 2.3, we briefly comment here on the other mechanisms at work.

High-frequency intra-molecular modes.– Intramolecular modes mostly occur at high frequencies, $\hbar\Omega_0 \sim 0.1 - 0.2eV$, originating from the stretching of the strong covalent bonds inside the molecule. The coupling to such modes, if sufficiently strong, can lead to the formation of small polarons, [42] i.e. the self-trapping of charge carriers by the molecular deformations that they themselves create upon residing on a given molecule: a simple argument predicts that when the energy gained upon such a local deformation — the relaxation energy E_P— is larger than the kinetic energy gained through delocalization on the periodic lattice, it becomes advantageous for the electron to remain localized on an individual molecule. Charge transport then occurs via hopping from site to site. Because at each hop the carriers must overcome an energy barrier proportional to the relaxation energy, the resulting mobility is exponentially activated with temperature.

There are two main reasons to exclude small polaron formation in high-mobility organic semiconductors. The most obvious is the experimental observation of "band-like" mobilities, i.e. which decrease with temperature instead of increasing as in the thermally activated behavior expected for small polarons. The second reason is that the calculated relaxation energies are insufficient to lead to small polaron formation in these materials: it is known theoretically that E_P decreases with the size of the molecules [6, 7], and the best organic semiconductors are typically constituted of "large" molecules. Furthermore, at the values of Ω_0 characterizing organic semiconductors, the naive estimate $E_P \simeq J$ for polaron formation is too optimistic, as phonon quantum fluctuations tend to delocalize the charges thus requiring a higher value of E_P in order to sustain a polaron. [43] The situation in the resulting intermediate regime of relaxation energies $E_P \sim J, \hbar\Omega_0$ cannot be described in simple terms, as it involves a subtle combination of coherent band transport and incoherent hopping (see e.g. [44, 45, 46] for numerical results). Although in selected temperature intervals the mobility around the polaron crossover could be compatible with the experiments, it is unlikely that the "universal" power-law behavior observed in experiments can be explained assuming that all compounds lie in such fine-tuned crossover regime. In the regime of parameters which applies to high-mobility organic semiconductors, high-frequency intra-molecular vibrations weakly affect charge transport via a modest renormalization of the effective mass [27, 47, 48, 49], but they are not the main limiting factor for the mobility.

Molecular polarization modes.– High-energy modes built from the electronic (excitonic) transitions in the molecules can also couple to the carrier motion. While resulting in an appreciable renormalization of the band parameters, [18, 50, 51] such polarization modes of electronic origin are too fast to efficiently couple to the carrier motion, and therefore do not directly affect the carrier lifetime and scattering time. We shall assume that molecular polarization effects are already included in the definition of the inter-molecular transfer integrals of the model Eq. (1).

Static disorder.– Because our focus here is on the *intrinsic* mechanisms limiting the mobility in organic semiconductors, we shall ignore the effects of structural disorder [13, 14, 15] or the influence of chemical impurities and polymorphs. As was studied systematically both theoretically [52] and experimentally [25], extrinsic sources of disorder can affect carrier transport even in the purest samples available nowadays, especially when these are placed in FET geometries. Static disorder causes the mobility to degrade at low temperature in the best cases, and wash out the intrinsic transport regime completely in the worst cases, leading to a thermally activated behavior. We shall however consider here an ideal situation where all extrinsic sources of disorder have been removed.

Substrate polarization.– It has been shown that the presence of a polarizable substrate can strongly affect the transport properties in field-effect transistors. The carriers couple electrostatically to the polarization of the substrate, which provides an additional source of electron-

phonon coupling, [53, 54] leading to the possible formation of Fröhlich polarons. In the static limit, the polarization acts instead as an additional source of disorder, due to the random arrangement of charged dipoles in the substrate. [55, 25] Both effects can convert the "band-like" temperature dependent mobility intrinsic to organic semiconductors into a thermally activated behavior, and will not be considered here.

2.3 A paradigmatic model

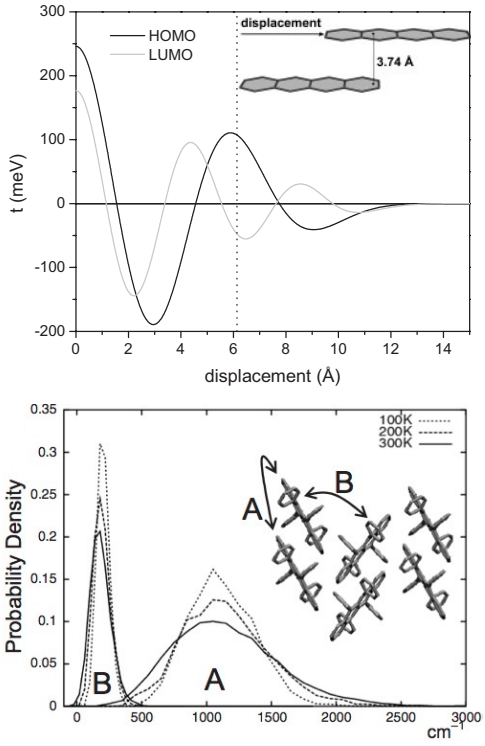

Figure 1: Top: Evolution of the HOMO and LUMO transfer integrals as a function of displacement, for a complex made of two tetracene backbones stacked along the rubrene a direction. The dotted line indicates the equilibrium displacement in the rubrene crystal (from Ref. [56]). Bottom: the distribution of transfer integrals between two different pairs of neighboring molecules in rubrene, calculated via molecular dynamics simulations, showing an essentially gaussian (thermal) probability (from Ref. [57]).

Low-frequency inter-molecular modes.– The coupling to inter-molecular vibrations — sometimes called the Peierls- or Su-Schrieffer-Heeger-type interaction — was considered already in the early days of organic semiconductors [5, 16, 17, 18, 19], and revived later with the advent of organic field-effect transistors [10]. It is however only recently that it has become a cornerstone in the understanding charge transport in organic semiconductors. There exist now a number of *ab initio* calculations of the precise values of such coupling by different methods and on different crystalline compounds (see e.g. Refs. [9, 28, 56, 58, 59, 60, 61]). Without going through a review of all the extensive theoretical literature on the subject, we highlight in Fig. 1 two observations which illustrate the essence of the microscopic mechanism and its implications.

Fig. 1 (top panel) shows the evolution of the HOMO and LUMO transfer integrals between two adjacent organic molecules as a function of their relative displacement, calculated at the INDO level in a geometry which corresponds to the crystal structure of rubrene (from Ref. [56]). The figure illustrates two important facts. The first is that the transfer integrals between π orbitals of neighboring molecules are typically on the order of $\sim 100meV$ or below, leading to narrow electronic bands whose width generally does not exceed $\sim 0.5eV$. The second is that they are strongly varying functions of the displacement, exhibiting oscillations which (in the case illustrated here) are directly related to the periodic structure of the phenyl groups in the molecular backbone. The strong dependence of the transfer integrals on the displacement signifies that the electrons on molecular orbitals are strongly coupled to the inter-molecular motions.

Fig. 1 (bottom panel) shows the statistical distribution of transfer integrals between HOMO orbitals of rubrene, also computed at the INDO level, obtained upon averaging over time on molecular dynamics simulations where the molecular positions in the crystalline matrix are allowed to thermally fluctuate (from Ref. [57]). The two nonequivalent transfer integrals denoted A and B exhibit essentially gaussian distributions of thermal origin, whose spread increases with temperature, and becomes comparable to the mean value itself in the experimentally relevant temperature range. Such large fluctuations, which are a key feature of organic solids, are a direct consequence of the weak van der Waals forces which bind the molecules together. As will be shown in the following paragraphs, it is precisely the anomalously large magnitude of such fluctuations which is responsible for the original transport mechanism that characterizes organic materials.

Model Hamiltonian.– The minimal model which accounts for the coupling to low-frequency molecular displacements in organic semiconductors can be written in second quantization as [11, 19, 62]

$$H = -J\sum_i [1-\alpha(u_i-u_{i+1})]\ (c_i^+ c_{i+1}+c_{i+1}^+ c_i)+H_{vib}, \quad (1)$$

with

$$H_{vib} = \sum_i \frac{M\omega_0^2}{2}u_i^2 + \sum_i \frac{p_i^2}{2M}. \quad (2)$$

The model is illustrated in Fig. 2.

The first term describes electrons with creation (annihilation) operators c_i^+ (c_i) hopping between molecular orbitals on neighboring sites along a one-dimensional chain (with lattice parameter a), which are treated in

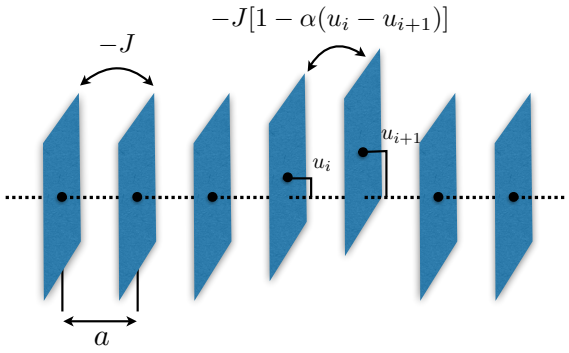

Figure 2: Illustration of the model Eq. (1). The transfer integral J between neighboring molecules is modulated by their relative displacement $u_i - u_{i+1}$ (readapted from [11]).

a tight-binding approximation as appropriate to narrow-band solids. The key ingredient of the model is that the amplitude J of inter-molecular transfer is modulated by the relative molecular displacements, $u_i - u_j$, as $J_{ij} = J[1-\alpha(u_i-u_j)]$. The coordinates u_i can represent in general either translational or rotational motions of the molecular units. It is customary to take the dependence of the inter-molecular transfer integrals on the molecular coordinates to lowest (linear) order. This is justified in the relevant regime of thermal molecular motions (the average molecular displacements are estimated to be of the order of $0.1\mathring{A}$ at room temperature, [23] to be compared with the scale of Fig. 1 (top)). As a consequence, deviations from linearity are weak, and are at the origin of the small deviations from the purely gaussian shape in the statistical distributions of Fig. 1 (bottom).

The second term, H_{vib}, describes the harmonic vibrations of the molecules around their equilibrium positions. The characteristic frequencies of the inter-molecular vibrations are in the range $\hbar\omega_0 \lesssim 10meV$. Such low values, which result from both the weak inter-molecular forces and the large weights of the moving molecular units, allow for a classical treatment of the molecular motions as long as $\hbar\omega_0 \lesssim k_B T$ (see below).

To the best of our knowledge, the above model was first introduced in the early days of organic semiconductor research in the k-space form Eq. (3) given below. [16, 17] The interaction term is formally analogous to the popular Su-Schrieffer-Heeger (SSH) model [63] that describes the properties of conjugate polymer chains, although it is applied here to a different physical situation. The first important difference is that in the SSH model, acoustic phonons are considered instead of the dispersionless vibrations of Eq. (3). The qualitative features of the model in the case of acoustic phonons are different, see e.g. Refs. [64, 65]. Secondly, here a low density of injected carriers is considered while in polymers the electron density is large and the electron system is degenerate (the bands are half-filled by construction, and the SSH interaction is itself responsible for dimerization of the structure and for the consequent opening of a gap at the Fermi energy). The final difference is quantitative, as both the inter-molecular transfer integrals J and the scale of the inter-molecular vibration frequencies in small-molecule organic semiconductors are more than one order of magnitude smaller than in polymers.

The electronic properties of the model Eq. (1) can be expressed in terms of the temperature T and two dimensionless coupling parameters: the electron-lattice coupling strength $\lambda = \alpha^2(\hbar/2M\omega_0)(J/\hbar\omega_0)$ and the adiabatic ratio $\hbar\omega_0/J$. Unless otherwise specified, we shall consider in what follows the values of microscopic parameters evaluated in Ref. [57] for the direction of highest conduction in rubrene, i.e. $J = 143meV$, $\omega_0 = 6.2meV$ ($\hbar\omega_0/J = 0.044$) and $\lambda = 0.17$, which fall in the typical range of parameters of high mobility organic semiconductors

3 Semi-classical and hopping theories

This Section presents a brief description of how standard approaches perform on the model Eq. (1). The results for the temperature dependence of the mobility, when available either in analytical or numerical form, are summarized in Fig. 3 and compared with existing measurements in rubrene FETs. Fig. 3 shows that "standard" methods generally overestimate the mobility: the values calculated at room temperature fall in the range $\mu = 50 - 200cm^2/Vs$, while the measured mobilities in rubrene are around $\mu = 10 - 20cm^2/Vs$. Such disagreement tells us that a fundamental mechanism of reduction of the mobility is missing in these theories. While one could try to bring the theoretical values closer to the experimental range by including a number of other interactions among the ones enumerated in Sec. 2.2, we find it unlikely that these effects will restore a proper agreement if they are treated correctly. As will become clear in Section 4, the failure of standard theories is due to the fact that they do not take quantum localization effects into account. Including these effects not only restores the quantitative agreement with the experimental mobilities, but also solves the experimental puzzles identified in the preceding Section concerning the duality between the extended and localized character of the charge carriers.

3.1 Semi-classical approaches

3.1.1 Band transport

Bloch-Boltzmann transport theory starts from the solution of the electronic problem in an unperturbed, perfect lattice. In this limit the electrons form Bloch waves identified by a well-defined momentum k and energy ϵ_k. Scattering to impurities or lattice vibrations is included

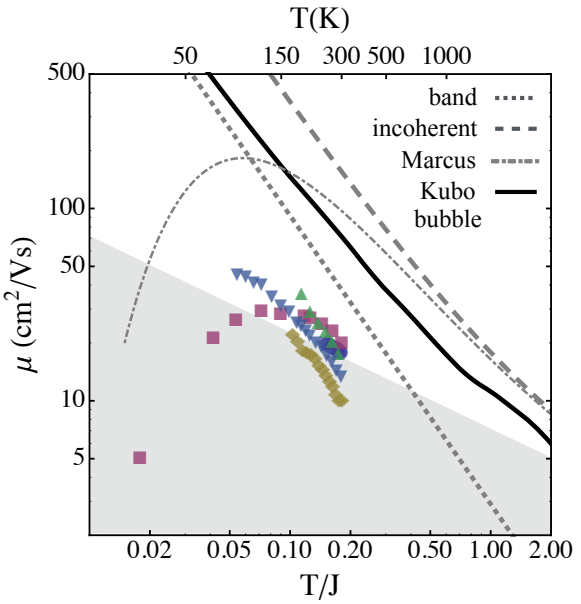

Figure 3: Mobility calculated from Eq. (1) using semi-classical and hopping theories: band theory, Eq.(7); incoherent limit, Eq. (14); Marcus theory, Eq. (15) and Kubo formula in the bubble approximation, Eq. (19). The microscopic parameters are those given at the end of Sec. 2.3. The gray shaded area shows the Mott-Ioffe-Regel limit defined by Eq. (11). The data points represent different experimental measurements on rubrene FETs: disks [66], squares [67], diamonds [34], up triangles [54], down triangles [68]. The theoretical curves all overestimate the experimental mobilities, suggesting that some important microscopic phenomenon is missing in the description.

as a perturbation, by introducing a transport relaxation time τ_k^{tr} for the Bloch eigenstates.

To work in momentum space, one proceeds by rewriting Eq. (1) as

$$H = \sum_k \epsilon_k c_k^+ c_k - \frac{1}{\sqrt{N}} \sum_{kq} g_{k,k+q} c_{k+q}^+ c_k (a_q^+ + a_{-q}) + \sum_q \hbar\omega_0 (a_q^+ a_q + 1/2) \quad (3)$$

with $\epsilon_k = -2J\cos ka$ the eigenenergies of the unperturbed one-dimensional chain, $g_{k,k+q} = 2ig[\sin(k+q)a - \sin ka]$ the Fourier transform of the electron-vibration interaction, with $g = (\alpha J)\sqrt{\hbar/(2M\omega_0)}$, and a_q^+, a_q the phonon creation and annihilation operators. Note that with these definitions, the dimensionless coupling constant takes the form $\lambda = g^2/(\hbar\omega_0 J)$.

In the Boltzmann description of electronic transport in nondegenerate semiconductors, the mobility is expressed as [69]

$$\mu(T) = \frac{e}{nk_BT} \sum_k v_k^2 \tau_k^{tr} e^{-(\epsilon_k - \tilde{\mu})/k_BT}, \quad (4)$$

where τ_k^{tr} and v_k are respectively the transport scattering time and the band velocity for electrons of momentum k, $\tilde{\mu}$ is the chemical potential and $n = \sum_k e^{-(\epsilon_k - \tilde{\mu})/k_BT}$ the thermal population of carriers. In the quasi-elastic limit where the phonon frequency sets the smallest energy scale in the problem, $\hbar\omega_0 \ll k_BT, J$ the scattering time is defined as

$$1/\tau_k^{tr} = \frac{2k_BT}{\hbar\omega_0} \int dq\, g_{k,k+q}^2 (1 - \cos\theta_{k,k+q})\, \delta(\epsilon_k - \epsilon_{k+q}) \quad (5)$$

with $\theta_{k,k+q}$ the angle between the incoming and outcoming momentum states. Reminding that the coupling matrix element $g_{k,k+q} \propto g$ and using the definitions given after Eq. (3), we see that the scattering rate $\hbar/\tau_k^{tr} \propto \lambda k_BT$ (cf. Ref. [62]). The present theory is consistent provided that the scattering rate is small compared to the bandwidth, i.e. $\lambda k_BT \ll J$.

The integral in Eq. (5) can be carried out analytically for the present model, yielding

$$\mu_{\rm band} = \frac{\mu_0}{16\pi\lambda} \frac{J}{k_BT} \frac{\sinh(2J/k_BT)}{I_0(2J/k_BT)}, \quad (6)$$

with I_0 the modified Bessel function. In the above expression, the absolute units of mobility are set by the prefactor $\mu_0 = ea^2/\hbar$, which equals $7cm^2/Vs$ in the direction of highest mobility of rubrene. Note that the above result can be straightforwardly generalized to the case of a finite vibrational frequency $\omega_0 \neq 0$, in which case the mobility is seen to rise exponentially at temperatures $k_BT \ll \hbar\omega_0$ due to the dispersionless (gapped) nature of molecular vibrations.

In the limiting cases of temperatures much lower or much higher than the bandwidth, the above expression reduces to the following power laws: [16, 17]

$$\mu_{\rm band} = \frac{\mu_0}{8\sqrt{\pi}\lambda} \left(\frac{J}{k_BT}\right)^{3/2} \quad k_BT \ll 2J \quad (7)$$

$$\mu_{\rm band} = \frac{\mu_0}{4\pi\lambda} \left(\frac{J}{k_BT}\right)^{2} \quad k_BT \gg 2J. \quad (8)$$

The low temperature result is illustrated as the dotted line in Fig. 3. The high temperature result is not shown, as it applies outside the relevant range in experimental systems: taking the representative value $J = 143meV = 1660K$ for rubrene from Sec. 2.3, the high temperature limit would apply at $T \gg 2J \sim 3000K$.

3.1.2 Mott-Ioffe-Regel condition

In the large scattering regime, the theory of band conduction presented above breaks down due to the progressive loss of momentum conservation. In non-degenerate semiconductors, this happens when the apparent mean-free-path ℓ for band electrons reduces to values comparable or below the inter-molecular spacing a. The Mott-Ioffe-Regel (MIR) condition $\ell \simeq a$ thus provides a lower bound for the applicability of Bloch-Boltzmann theory.

To determine the value of the mobility corresponding to the MIR condition, we start from the semi-classical Drude expression

$$\mu = \frac{e\tau}{m^*}. \tag{9}$$

Introducing the mobility units $\mu_0 = ea^2/\hbar$ and the band mass $m^* = \hbar^2/(2Ja^2)$ for the considered one-dimensional lattice, we rewrite Eq. (9) as

$$\mu = \mu_0 \frac{2J}{(\hbar/\tau)}. \tag{10}$$

We now recall that the mean-free-path is the length over which the carriers diffuse between successive scattering events separated by τ, which can be written as $\ell \sim \sqrt{D\tau}$, with D the diffusion constant. Using the semi-classical expression $D = \langle v^2 \rangle \tau$ and the equipartition principle $\langle v^2 \rangle = k_B T/m^*$, and imposing the condition $\ell/a = 1$ we arrive at

$$\mu_{MIR} \sim \mu_0 \left(\frac{2J}{k_B T} \right)^{1/2}, \tag{11}$$

which is illustrated in Figs. 3 and 5. Even in a "high mobility" organic semiconductors such as rubrene, the condition $\mu > \mu_{MIR}$ is experimentally violated at room temperature. Taking $J = 143meV$ and $T = 300K$ yields a MIR value $\mu_{MIR} \simeq 23cm^2/Vs \simeq 2\mu_0$. This corresponds to the typical experimental values in rubrene clean samples, which are precisely in the range $10 - 20cm^2/Vs$. A similar estimate was obtained in Ref. [71] based on the actual band structure of oligoacene crystals (see also [47, 70] for a calculation of the scattering time). Comparing this estimate with Eq. (10) above we see that the MIR condition roughly coincides with the condition that the elastic scattering time becomes shorter than the intermolecular transfer time, $\tau \lesssim \hbar/J$. [70]

We also mention here that the breakdown of Bloch-Boltzmann theory and the resulting resistivity saturation has been thoroughly explored in the case of degenerate systems, leading to the concept of "bad metals" (cf. Refs. [72, 73]). In that case the MIR condition becomes $\ell \simeq 1/k_F$ instead of $\ell \simeq a$, with k_F the Fermi wavevector.

3.1.3 Fully incoherent limit

The semi-classical transport theory was generalized to the large scattering case by Gosar and Choi [18] and later by Sumi, [74] based on the Kubo formula for the electrical conductivity. [75, 69] These authors observed that, even remaining in the spirit of semi-classical transport which neglects quantum localization effects altogether (see below and Sec. 4), a different regime of charge transport sets in when the fluctuations of the transfer integrals exceed their mean value J, where the bands themselves are no longer well-defined.

The transfer integrals fluctuate as a direct consequence of the thermal molecular motions, as encoded in Eq. (1). To estimate their spread we observe that in the harmonic approximation each vibrational mode u_i is gaussianly distributed with fluctuations proportional to $k_B T$. Treating u_i and u_j as independent variables, and collecting the numerical factors, yields for the inter-molecular transfer integrals J_{ij} a gaussian distribution whose variance is $s^2 = 4\lambda J k_B T$. The condition for fully incoherent transport is therefore $s \gtrsim J$, i.e. $k_B T \gtrsim J/(4\lambda)$, which is opposite to the band-transport condition given before Eq. (6).

Although it is true that thermal molecular fluctuations are large in organic semiconductors, this extreme limit is never reached experimentally. For example, taking $J = 1660K$ and $\lambda = 0.17$ for rubrene from Sec. 2.3 implies that the fully incoherent limit would be reached for $T \gtrsim 2500K$. It is however important to describe this mechanism here because, as will be shown via the comprehensive treatment of Sec. 4.1, both the diffusion of incoherent states and the coherent transport of Eq. (7) are predicted to participate to semi-classical charge transport at the experimentally relevant temperatures.

In the limit $s \gg J$, the weakly scattered Bloch waves with a well-defined momentum k that enter into Eq. (4) are replaced by a fully incoherent density matrix describing a diffusion from site to site as in a classical random walk. In mathematical terms, the fact that all informations on the energy dispersion of momentum states are lost translates into the fact that the spectral function $\rho(k, \omega)$ describing the quasiparticle excitations becomes k-independent, i.e. $\rho(k, \omega) \to \rho(\omega)$. The spectral function becomes a local quantity, signalling the loss of coherence between different molecular sites. It can be easily shown that it tends to a gaussian of variance $s^2 = 4\lambda J k_B T$ itself [18, 74]

$$\rho(\omega) = \frac{1}{\sqrt{2\pi s^2}} e^{-\omega^2/2s^2}. \tag{12}$$

This spectral function can be directly inserted in the Kubo formula [75, 69], in the simplest approximation where the current-current response function is taken to be a convolution between two single-particle propagators — the so-called "bubble" form [44]. This yields the following mobility:

$$\mu_{\rm inc} = \mu_0 \frac{\pi \langle J_{ij}^2 \rangle}{x k_B T} \int d\omega \rho(\omega)^2 e^{-(\omega - \tilde{\mu})/k_B T} \tag{13}$$

with $x = \int d\omega \rho(\omega) e^{-(\omega - \tilde{\mu})/k_B T}$ the thermal population of non-degenerate carriers, $\tilde{\mu}$ being the chemical potential. The prefactor $\langle J_{ij}^2 \rangle = J^2(1 + 4\lambda k_B T/J)$ accounts for the temperature dependence of the mean square of the inter-molecular transfer integrals. Its increase with respect to the reference value J^2 represents the thermally assisted tunneling processes caused by the fluctuations of the molecular positions, which set in and favor incoherent hopping at temperatures $k_B T \gtrsim J/4$, i.e. essentially where the present incoherent limit applies. The importance of such vibrationally-assisted hopping was first recognized by Gosar and Choi in Ref. [18].

Performing the integral above leads to

$$\mu_{\rm inc} = \mu_0 \sqrt{\frac{\pi}{8\lambda}} \left(\frac{J}{T}\right)^{3/2} \left(1 + 4\lambda \frac{k_B T}{J}\right). \qquad (14)$$

Similarly to the band conduction of Eqs. (7) and (8), the fully incoherent diffusion mechanism of Gosar and Choi also results in a metallic-like, power-law temperature dependence of the mobility, which is displayed in Fig. 5 as a dashed line. In the high temperature regime where the fully incoherent limit applies, the power law $\sim T^{-3/2}$ that comes from the progressive energy spread of electronic states (the first term in Eq. (14)) is converted into $\sim T^{-1/2}$ due to phonon-assisted tunneling.

We stress here that although Eq. (14) describes a regime where band transport is completely destroyed, it remains essentially a semi-classical approximation to charge transport. The semi-classical nature of the theory is implicit in having expressed the Kubo formula in Eq. (13) as a convolution integral, therefore neglecting all particle-hole interferences (the so-called vertex corrections) which are responsible for quantum localization processes. [12]

3.2 Hopping and polaron-based theories

The failure of semi-classical approaches and the evidence of short mean-free-paths has been traditionally considered as an indication of polaronic localization of the carriers, which has led to the widespread application of hopping transport theories to crystalline organic semiconductors. Such theories have been used despite the fact that, as was noted in Sec. 2.2, for polaronic localization to occur the polaron energy should be the largest scale in the problem, which is not the case for the most conductive organic crystals such as pentacene or rubrene. [47, 76] We review here the predictions of these approaches when applied to the model Eq. (1).

3.2.1 Marcus theory

Marcus theory describes the hopping motion of charge carriers which are self-trapped by their induced molecular deformations. The corresponding mobility is calculated starting from the transfer rate between two adjacent molecules, assuming that the quantum coherence is lost after each hopping event, and takes the following thermally activated form:

$$\mu(T) = \mu_0 \ \langle J_{ij}^2 \rangle \left(\frac{\pi}{4\varepsilon_r (k_B T)^3}\right)^{1/2} e^{-\varepsilon_r / 4 k_B T}. \qquad (15)$$

The quantity $\varepsilon_r = 2\lambda J$ is the inter-molecular reorganization energy, which determines the energy barrier, and is proportional to the coupling constant λ ($\varepsilon_P = \varepsilon_r/2 = \lambda J$ is the corresponding relaxation energy associated to intermolecular vibrations). As in Eq. (14), $\langle J_{ij}^2 \rangle$ is the mean square of the inter-molecular transfer integrals, and we have specialized to one space dimension. This behavior is illustrated in Fig. 3 as a dash-dotted curve.

Marcus theory relies on the assumption that the molecular energy scales (in the present case the inter-molecular relaxation energy ε_P and vibrational energy $\hbar\omega_0$) are much larger than the transfer integral J. Even when these conditions are not fulfilled, however, Eq. (15) exactly recovers the incoherent conductivity Eq. (14), provided that the temperature is much higher than the activation barrier, $k_B T \gg \varepsilon_r/4$ (cf. Fig. 3, where $\varepsilon_r/4 = 0.085J$). This agreement with semi-classical transport theory at high temperatures provides it with a certain interpolating power and somehow justifies its use when addressing qualitative trends between different compounds. [29]

We note that Eq. (15) is formally equivalent to the mobility obtained in small polaron theory within the so-called Holstein molecular crystal model [42] in the non-adiabatic limit $J \ll \hbar\omega_0$ and at sufficiently high temperatures, $k_B T \gg J$. For an overview of the different transport regimes of small polarons we refer the reader to Refs. [44, 46, 77].

3.2.2 Small polaron theory and extensions

Early theories of small polaron transport based on the local Holstein-type coupling [42] have been adapted to non-local electron-phonon coupling typical of organic systems [59, 78, 79]. In a series of works [58, 59, 79] a power law behavior $1/T$ of the mobility has been predicted to occur under the conditions that the electron-phonon coupling is not too large and that the activated regime is not reached in the temperature range of interest. In subsequent works [80, 81] the theory has been extended to recover the weak coupling case as a limiting behavior. A careful analysis of the terms arising from the structure of the current-current correlation function allows to separate a coherent and an incoherent contribution. The sum of these two contributions can yield a power-law different from $1/T$.

To critically examine these theories and their possible application to organics we need to go further into the technical details of the calculations. To this aim we follow the treatment of Ref. [59] and adapt it explicitly to the model Hamiltonian Eq. (1) by formulating it in real space. All the above theories are ultimately based on the so called polaron [42] or "Lang-Firsov" transformation, [82, 83] generalized to q-dependend electron-phonon matrix elements as in Eq. (3). Such transformation is devised to formally cancel the electron-vibration interaction term in the Hamiltonian, which is achieved by changing the electron operators into "dressed" polaron operators and shifting the phonon operators by a constant term. This is done in practice by introducing the

unitary trasformation $U = e^S$ where

$$\begin{aligned} S &= -\sum_{<i,j>} s_{i,j} c_i^\dagger c_j \\ s_{i,j} &= \sum_q g_q^{i,j} (a_q - a_{-q}^\dagger) \\ g_q^{i,j} &= \frac{1}{N\omega_0} \sum_k g_{k,k+q} e^{ik(R_j - R_i)} e^{-iqR_i}. \end{aligned} \tag{16}$$

The transformed Hamiltonian can be rewritten in terms of the original operators as

$$UHU^\dagger = -\sum_{i,j} \bar{J}_{i,j} c_i^\dagger c_j + \omega_o \sum_q a_q^\dagger a_q + H_{res} \tag{17}$$

where $\bar{J}_{i,j} = J \sum_{k,l} [e^{-s}]_{i,k} c_k^\dagger c_l [e^s]_{l,j} + \delta_{i,j} \varepsilon_P$ contains a renormalized kinetic energy operator and a polaronic shift in the energy (s being the matrix whose elements $s_{i,j}$ are defined in Eq. (16)).

Contrary to the original Lang-Firsov transformation applied to the case of local Holstein-type coupling, Eqs. (16) are non-local, and do not entirely remove the electron-phonon interaction because they do not yield a simple shift of the phonon operators. Indeed, we have $U a_q U^\dagger = a_q + \sum_{i,j} [s, a_q]_{i,j} c_i^\dagger c_j + \Delta a_q$ where the shift is $[s, a_q]_{i,j} = \frac{g_{-q}^{i,j}}{\omega_0}$ and Δa_q contains non-linear terms in the phonon operators a_q and $a_q^\dagger$ (a similar equation holds for a_q^+). These are responsible for the residual term H_{res} in Eq. (17). This term has been argued to be irrelevant provided that the electron-phonon coupling is not too large [84] and it is usually neglected in the polaronic treatment of the mobility. [59]

The kinetic energy terms in Eq. (17) contain phonon operators to all orders in $g_{k,k+q}$, which cannot be treated exactly (this is where the unitary transformation has moved the original interaction terms). The next step in the calculation is thus to implement an approximation devised by Holstein [42] which treats the polaron kinetic energy by averaging the phonons over their thermal state. This leads to the following renormalized band dispersion:

$$\bar{\epsilon}_k = \frac{1}{\sqrt{N}} \sum_{i,j} e^{-ik(R_i - R_j)} \sum_{<n,m>} \langle [e^s]_{i,n} [e^{-s}]_{m,j} \rangle. \tag{18}$$

A further common approximation is to take only the nearest neighbor terms in the sum of Eq. (18). The renormalized band dispersion resulting from Eq. (18) has been evaluated using realistic band structure parameters obtained from density functional theory (DFT) in Ref. [59]. The main qualitative results are basically the same as obtained in the model Hamiltonian Eq. (1), and which are well known since the works of Holstein: above a crossover temperature $k_B T_c \simeq \hbar\omega_0$, the coherent polaron bandwidth decreases with temperature due to the exponential factors in Eq. (18).

The calculation of the mobility now proceeds through the Kubo formula [69, 75] (see e.g. Refs. [42, 81]). Due to the decoupling between polaron and phonons achieved by Eq. (17), the current-current correlation function is factored into products of bosonic and fermonic correlators. We can write schematically $\langle \hat{J}(t) \hat{J}(0) \rangle = \langle \hat{B}(t) \hat{B}(0) \rangle \langle \hat{J}^{(p)}(t) \hat{J}^{(p)}(0) \rangle$, where the $\hat{B}(t)$ contain only phonon operators and $\hat{J}^{(p)}(t)$ is the polaron current operator. The same structure applies to the single particle propagator, as shown in Ref. [85]. Writing $\langle \hat{B}(t) \hat{B}(0) \rangle = \langle \hat{B}(t) \hat{B}(0) \rangle - \langle \hat{B}^2(0) \rangle + \langle \hat{B}^2(0) \rangle$ it is possible to recast the current-current correlator as as a sum of two contributions: (i) a coherent part which is that of unscattered free polarons, $\langle \hat{B}^2(0) \rangle \langle \hat{J}^{(p)}(t) \hat{J}^{(p)}(0) \rangle$, and which incorporates the terms responsible for the band-narrowing; (ii) a remainder interpreted as an incoherent part which includes polaron-phonon scattering. At this level of approximation, i.e. as long as H_{res} is neglected, the polaron-phonon scattering comes from the time dependence of the bosonic operators $\hat{B}(t)$, which however does not enter in the coherent part. As a consequence, the latter is formally divergent and an *ad hoc* regularization parameter must be introduced in the theory. [42, 81] When this is done, a crossover between the two contributions (i) and (ii) occurs as the temperature increases above $k_B T \simeq \hbar\omega_0$). When calculated for the typical intramolecular modes in organic semiconductors, this locates the crossover around $50 - 100K$ [80] so that at room temperature the transport is mainly dominated by the incoherent contribution.

We have to stress that the above mentioned *ad hoc* regularization of the coherent transport contribution will inevitably affect the quantitative results for the mobility. A more sophisticated treatment which porperly incorporates the missing scattering effects in the case of the Holstein model and can be found in Ref. [44], showing that the mobility is finite without the need to introduce extra phenomenological terms in the Hamiltonian. To the best of our knowledge, an analogous treatment for the Peierls-type coupling of Eq. (1) hasn't been developed yet.

In addition to the above mentioned *ad hoc* regularization procedure, there is another fundamental issue which is often neglected in the application of theories based on the polaron transformation, and it is related to the Holstein band narrowing approximation Eq. (18). Studies have been performed to assess the validity of such approximation scheme, both at zero temperature via numerical Monte Carlo calculations combined with an analytical expansion in powers of $1/\lambda$, [86] and at finite temperature using a generalization of the so-called momentum-average approximation [87] to non-translationally invariant systems. [48] Such studies have shown that, as was originally devised by Holstein, the band-narrowing approximation can only be applied if the vibrational frequencies are much larger that the unrenormalized electron bandwidth (the so called anti-adiabatic limit, $J \ll \hbar\omega_0$), because only in this case the phonon cloud can instantaneously re-arrange to follow the motion of the carriers as encoded in Eq. (18). Unfortunately this is not

the case for the inter-molecular vibrations relevant in organic semiconductors, [9, 28, 56, 58, 59, 60, 61] which lie in the opposite adiabatic regime where the electrons can follow instantaneously the slow motion of the molecules. Even in this case, it has been shown that the intermolecular coupling is not sufficient to form an inter-molecular (bond-centered) polaron. [47, 64, 94]

We mention that ARPES experiments on Pentacene films, which reported a bandwidth reduction upon increasing temperature, were initially interpreted according the concept of polaron band narrowing, in apparent support to polaron theories for the mobility. [88] These measurements, however, were subsequently re-examined showing that the observed band narrowing can actually be explained by accounting for the expansion of the molecular lattice with temperature. [49, 89, 90]

4 The transient localization scenario

In the preceding Sections we have listed a series of open experimental issues in organic semiconductors, and shown that these cannot be explained by conventional theories of charge transport. We anticipated that the cause of the puzzling experimental observations should be seeked in the existence of large amplitude thermal molecular motions, which act as a source of dynamical disorder for the charge carriers. This causes a quantum localization of the wavefunctions on timescales shorter than the period of molecular oscillations, strongly limiting the carrier diffusion. In this Section we describe the theoretical framework and numerical methods that have been developed in recent years in order to properly address the transport properties in this original regime of *transient localization* that is characteristic of organic semiconductors.

4.1 Reconciling the band-like / localized carriers duality.

We have seen in Section 3.1 that, within semi-classical transport theory, two very different transport mechanisms are realized in the limits where the fluctuations s of the inter-molecular transfer integrals are either much smaller or much larger than the equilibrium value J characterizing the perfect crystal. In the first case, transport is dominated by the diffusion of extended carriers with well-defined momentum, leading to Eq. (7). In the second case, itinerant carriers are washed out and charge transport occurs via incoherent states diffusing from site to site, leading to Eq. (14).

These two apparently contradictory views can be reconciled by properly addressing the properties of the electronic states as a function of their energy and momentum. This was done in Refs. [62] and [52] by solving exactly the model Eq. (1) in the limit of static molecular displacements. This limit, where thermal fluctuations are treated as a statistical disorder in the inter-molecular bonds, provides a very accurate description of the excitation spectrum and carrier lifetimes in the low vibrational frequency regime appropriate to organic semiconductors. More importantly, it gives fundamental informations on the localization of the electronic states.

The results obtained in Refs. [52, 62] have shown that at intermediate values of the ratio s/J, corresponding to the experimentally relevant temperature range, both extended "band-like" carriers and incoherent excitations coexist *in different regions of the excitation spectrum*: carriers with a markedly itinerant character are mostly located within the bulk of the band, while the most dramatic effects of inter-molecular fluctuations are instead concentrated around the band tails, where they cause the states to have a more localized character. The origin of the long-standing controversy on the microscopic identity of the charge carriers in organic semiconductors comes from the fact that different experimental probes will see alternatively one feature or the other, or a mixture of both.

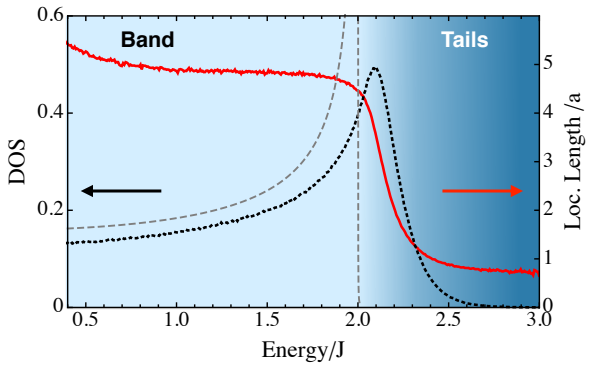

Figure 4: Density of states (black dotted, left axis) and energy-resolved localization length in units of the lattice spacing (red, right axis) DOS obtained by exact diagonalization of Eq. (1) in the limit of static displacements. The data correspond to the top of the HOMO band and are calculated for a coupling constant $\lambda = 0.17$ at $T = 0.3J$ (from Ref. [52]). Tails of localized states with spread $\approx a$ emerge beyond the band edge, whose width is controlled by the temperature via the parameter $s = \sqrt{4\lambda J k_B T}$. This parameter also controls the spatial extension of the band states, which rapidly decreases with temperature but remains larger than the lattice spacing throughout the experimentally relevant temperature regime.

The incipient localization length.– Fig. 4 reports two quantities which illustrate the duality between itinerant and incoherent carriers. The dotted line is the density of states (DOS) $\rho(\nu)$ at the top of the HOMO band obtained from the static solution of Eq. (1) (number of states per unit volume and unit energy J). The DOS of a perfectly ordered one-dimensional crystal is shown for reference (dashed). Including the thermal inter-molecular

fluctuations has two visible effects. First, the edge of the band at $\nu = 2J$ is rounded off and shifts to higher energy, indicating an increase of the effective bandwidth. This follows from the fact that $\langle J_{ij}^2 \rangle > J^2$, as reported after Eq. (13). Second, a tail of new states is generated beyond the range of band states. Both effects are controlled by the amount of inter-molecular fluctuations, quantified through the spread $s = \sqrt{4\lambda J k_B T}$ introduced previously. In particular, the width of the tails is directly proportional to s and therefore increases with temperature.

The crucial information on the localized character of the states comes from the red curve in Fig. 4, which illustrates the spread of the electronic wavefunctions as a function of their energy in the excitation spectrum. Such quantity was introduced in Ref. [62] in order to rationalize the idea of an underlying finite localization length for electrons proposed in Ref. [11] (see Section 4.2), and is now commonly used in model theoretical studies of organic semiconductors, see e.g. Refs. [22, 52, 76, 91]. The idea is that the system in the presence of slow molecular motions (where the charge carriers are mobile as clearly shown by experiments) retains some important characteristics of the static disorder problem, where all electronic states would instead be localized. In particular, the localization length calculated in the static disorder problem is reflected as an "incipient" localization length in the dynamical case, [52, 70, 92] in a sense that will be rigorously defined in Sec. 4.3.

The comparison with the DOS allows us to identify two distinct regions in the electronic spectrum, separated by a crossover region of width $\simeq s$ around the band edge. States located in the bulk of the band extend over many inter-molecular distances at low temperatures (their spatial extent is progressively reduced upon increasing the thermal disorder, also controlled by s). Tail states induced by disorder beyond the band edge instead have a much more local character, residing essentially on one molecular unit. The relative importance of these two types of excitations is subtly controlled by the temperature: on one hand, the amount of thermal molecular motions controls the emergence of tail states and the progressive destruction of quasi-particle band states; on the other hand, the temperature also controls the relative weight of these states, via their statistical population in the respective energy ranges. [52]

Kubo formula in the bubble approximation.– While the results presented above provide an essentially exact description of the properties of the electronic states, more input is required in order to assess how these single-particle states participate in the transport mechanism, which involves a two-particle correlation function. [75, 69] To this aim, an approximate treatment was developed in Refs. [62] and [52], which starts from the exact numerical calculation of the Green's function in the static disorder limit and assumes a convolution form for the current-current correlation function in the Kubo formula as in Eq. (13). The corresponding mobility can be written in compact form as [44, 52, 62]

$$\mu = \frac{e}{k_B T} \frac{\int d\nu e^{-\beta\nu} B(\nu)}{\int d\nu \rho(\nu) e^{-\beta\nu}}, \tag{19}$$

where $\rho(\nu) = \mathrm{tr}\hat{\rho}(\nu)$ is the interacting DOS with $\hat{\rho}(\nu) = -Im(\nu - \hat{H})^{-1}/\pi$. The function $B(\nu)$, which is proportional to an energy-resolved diffusivity, is defined in terms of the current operator $\hat{J}$ as

$$B(\nu) = \frac{\pi}{e} \mathrm{tr}[\Big\langle \langle\hat{\rho}(\nu)\rangle \hat{J} \langle\hat{\rho}(\nu)\rangle \hat{J} \Big\rangle] \tag{20}$$

where the trace is performed over lattice sites and angular brackets represent averages over the classical phonon field. This approach is more general than the one presented in Sec. 3.1.3, as it includes the full momentum and energy dependence of the electronic spectral function. In particular, it is able to describe the simultaneous presence of both band and incoherent states, acting as two complementary transport channels.

The results for the mobility obtained by this method are reported in Fig. 3 (full line). The calculated mobility interpolates smoothly between the two semi-classical limiting behaviors presented in Section 3.1: the transport is essentially governed by band-like carriers at low temperature, i.e. when thermal molecular disorder is small, corresponding to Eq. (7); upon increasing the temperature, the relative weight of the incoherent states progressively increases up to the point where band states get completely washed out, as their lifetime becomes shorter than the inter-molecular transfer time. The mobility then tends to the fully incoherent expression Eq. (14).

Importantly, Fig. 3 shows that the present treatment, albeit more sophisticated than the ones of Section 3.1, is still unable to restore a quantitative agreement with the experiments. This failure in reproducing the experimental results indicates that localization effects in organic semiconductors are stronger than what can be included in any extension of semi-classical theory.

4.2 Ehrenfest simulations

The pioneering work of Troisi and Orlandi in 2006 [11] suggested the possibility that the carriers in organic semiconductors undergo some form of localization due to the strong scattering introduced by the large molecular motions. These authors started from the idea that because molecular motions are slow, they can be treated classically and separated from the faster electronic motion in a Born-Oppenheimer scheme. Accordingly, they performed numerical simulations where the electronic problem in Eq. (1) is solved exactly at each instant of time following the classical evolution of the slow degrees of freedom $\{u_i\}$, through the Ehrenfest method. We summarize this method here, following the description given in Ref. [92].

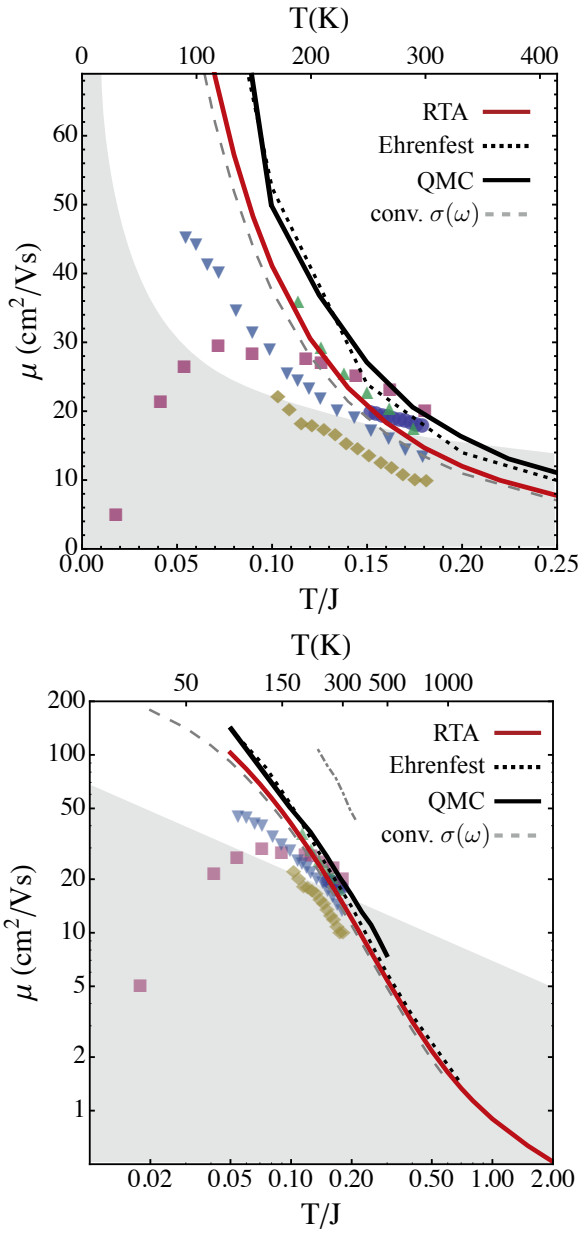

Figure 5: Top: Mobility calculated from Eq. (1) using theories which account for quantum localization processes: RTA, Ehrenfest simulations, QMC and Lorentzian convolution of the optical conductivity (see text). The symbols for the experimental data are the same as in Fig. 3. The gray shaded area shows the Mott-Ioffe-Regel limit defined by Eq. (11). Bottom: same data, plotted in log scale, for a direct comparison with Fig. 3. The dash-dotted line is the Ehrenfest result of Ref. [57].

The coupled equations of motion for the electrons and molecular degrees of freedom read:

$$i\hbar\partial_t|\Psi,t\rangle = H_{el}(\{u_i\})|\Psi,t\rangle \quad (21)$$

$$\ddot{u}_i = -\omega_0^2 u_i - \frac{\partial}{\partial u_i}\langle t,\Psi|H_{el}(\{u_i\})|\Psi,t\rangle, \quad (22)$$

where H_{el} is the electronic part of Eq. (1). In the Ehrenfest method, the transport properties are calculated by tracking the quantum spread of the electronic wavefunction as the mean-square displacement $\Delta X^2(t) = \langle\Psi|[\hat{X}(t) - \hat{X}(0)]^2|\Psi\rangle$ in real time, as illustrated in Fig. 6(a) (readapted from [92]). This is done by following simultaneously the evolution of the state vector $|\Psi,t\rangle$ and that of $|x\Psi,t\rangle$, which is the evolution of the state $\hat{X}|\Psi,0\rangle$. The quantum spread is then given by $\Delta X^2(t) = \langle t,x\Psi|x\Psi,t\rangle + \langle 0,x\Psi|x\Psi,0\rangle - 2Re\langle t,x\Psi|x\Psi,0\rangle$. The time derivative of the spread directly provides the instantaneous diffusivity $D(t) = d\Delta X^2(t)/2dt$ (Fig. 6(b)). The mobility is then extracted from the diffusivity in the long time limit $D = \lim_{t\to\infty} D(t)$ through the Einstein formula, $\mu = eD/k_BT$. [75]

Finite temperature simulations are performed starting from a thermal state of the classical oscillators and taking the initial state of the electron as an eigenstate of H_{el} in the corresponding distorted landscape, with a probability proportional to the Boltzmann weight. Since the initial oscillator state has no polaronic disortion in it, the (small) initial correlations between the charge and the lattice degrees of freedom are lost in the dynamical evolution. Starting instead from a localized electron-lattice correlated polaronic initial state, these correlations are preserved at least at low temperature by the Ehrenfest dynamics. [93] This case, however, does not apply here: for the model Eq. (1) a polaronic ground state can only be found for $\lambda \geq 0.5$, [64, 94] which is well above the values typical for organic crystals.

Beyond semi-classical transport.– The key advantage of the Ehrenfest method over previous approaches of charge transport in organic semiconductors is that it is able to account for quantum localization corrections in the sense of Anderson, because the electronic degrees of freedom are treated exactly. In other words, these mixed quantum-classical simulations are not "semi-classical" from the point of view of electronic transport. For this reason, and because they provide a direct way of visualizing the dynamics of charge carriers, Ehrenfest simulations have been extensively used in recent years both for one-dimensional and two-dimensional models for organic semiconductors. [11, 32, 52, 57, 76, 92, 93, 95, 96, 97, 98, 99, 100]

A close look at Fig. 6(a) shows that the behavior of the time-dependent electronic spread calculated with the Ehrenfest method is quite different from what would be expected from semi-classical diffusion. In semi-classical transport, the electronic wavefunction spreads ballistically at initial times, as $\Delta X^2(t) = \langle V^2\rangle t^2$, up to some characteristic scattering time τ where a diffusive behavior, $\Delta X^2(t) = (D_{sc}/2)t$, sets in (this behavior corresponds to the dashed line in Fig. 8 below). [52, 70, 92] Correspondingly the instantaneous diffusivity $D(t)$ would increase linearly at short times and then saturate to its long time limit D_{sc} at $t \gg \tau$. What is observed instead is

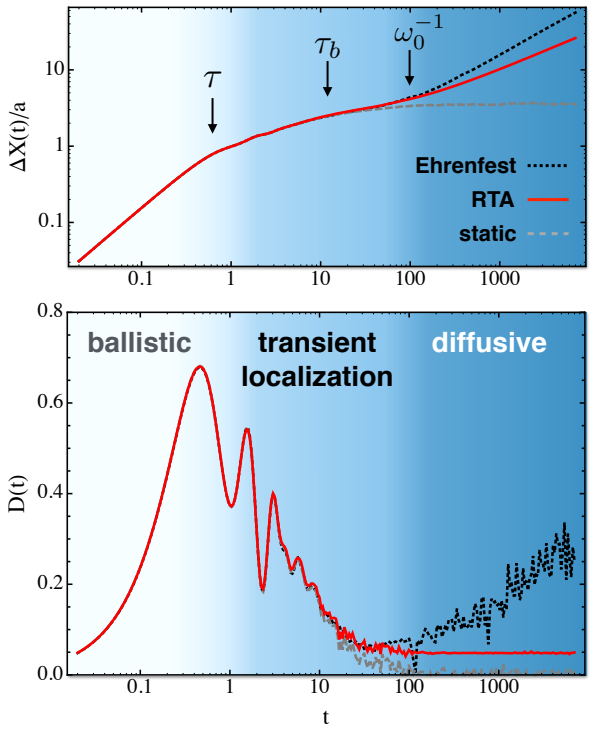

Figure 6: Top: time-dependent quantum spread of the electronic wavefunction, $\sqrt{\Delta X^2(t)}$, calculated for the model Eq. (1) via the Ehrenfest method (black dotted curve) and via the RTA by setting $\tau_{in} = \omega_0^{-1}$ (red curve). The result for static molecular displacements is shown for comparison (gray dashed). Bottom: the corresponding instantaneous diffusivity $D(t) = d\Delta X^2(t)/2dt$. The parameters are $J = 110meV$, $\lambda = 0.25$, $\omega_0 = 0.01J$, $T/J = 0.2$ (readapted from Ref. [92]). Time is expressed in units of $\hbar/J$.

that, after the initial ballistic behavior, the mean-square displacement of the electron bends down and tends to saturate at a time $\tau_b > \tau$, before diffusing again at a subsequent time τ_{in}. As a result, the diffusivity goes through a maximum and then decreases indicating the onset of localization. This decrease goes on up to the time $t \sim \tau_{in}$. The resulting diffusivity is considerably lower than the semi-classical value D_{sc}, which roughly corresponds to the maximum of $D(t)$. This peculiar non-monotonic behavior of the diffusivity identifies the transient localization mechanism for charge transport.

Comparing the numerical results at different values of the inter-molecular vibration frequencies shows that the time where the diffusion is restored is directly proportional to the timescale of molecular motions, $\tau_{in} \sim 1/\omega_0$. [92] The behavior at times $t \lesssim \tau_{in}$ is indistinguishable from what would be obtained in the presence of static molecular displacements (dashed curve in Fig. 6(a)), because the molecular motions effectively appear as frozen at such short time-scales. The behavior of the dynamically disordered system therefore "knows" about the existence of quantum localization processes and of a finite localization length for the electrons, even though a diffusive behavior is eventually obtained at times $t \gtrsim \tau_{in}$.

Drawbacks.– Despite its popularity, the Ehrenfest method suffers from a number of drawbacks. The first originates from the fact that the back-action of the electrons on the molecular motions is treated at mean-field level, in the form of an average instantaneous force (cf. Eq. (22)). It is known [45, 92, 101] that this back-action is not sufficient to thermally equilibrate the system, and results in a progressive heating of the electronic system due to the excess energy being constantly injected by the molecular vibrations. The consequences are visible in Fig. 6(b) (black dotted line): the diffusivity is not constant at long times, but increases steadily due to heating, because more and more conducting states within the band are artificially populated. This can lead to an over-estimate of the mobility that spuriously depends on the simulation time, which could be at the origin of the discrepancy between the results of [57] and those obtained by other authors using the same Ehrenfest method. To illustrate this point, in Fig. 5 we compare the data of Ref. [57] (dash-dotted line) with the data obtained by the same method and for the same set of parameters in Ref. [52] (dotted line), but with the prescription of evaluating the diffusivity at a fixed time $t = 1/\omega_0$: the mobility is much lower in the latter case, and is extremely close to the fully quantum calculation of Ref. [102] (see Sec. 4.4 below).

Also due to the average nature of the back-action term, the Ehrenfest method does not give access to the thermally activated mobility of finite-radius polaronic states. For polarons to be formed (and stable in a dynamical evolution) a feedback to the oscillator motion which goes beyond the average Ehrenfest method is needed. Starting from a localized electron-lattice correlated polaronic initial state a small-polaron evolution can be followed for limited times in the Ehrenfest dynamics. [93] However the averaged oscillator dynamics of the Ehrenfest method cannot sustain polaronic correlations in the long time limit even at large values of the electron-phonon coupling, unless the temperature is sufficiently small. This drawback was corrected by Wang and Beljonne in Ref. [45] by introducing surface hopping methods which go beyond the mean field character of the Ehrenfest average force (see Sec. 4.4).

The third issue is that wavefunction-based simulations cannot distinguish between the evolution of a state of finite radius whose center of mass diffuses over time (as in a classical random walk) and an evolution where the wavefunction itself spreads over time, unless the electron-phonon interaction has a large local contribution as in Ref. [93]. For the electron-phonon couplings typical of organics crystals, it is rather the spread ΔX^2 of the wavefunction *for a single initial set* of molecular displacements which grows with time, leading to a fully delocalized wavefunction in the long time limit (see Ref. [103] for an approach which includes decoherence in order to solve

this issue). The interpretation of the time snapshots of the electronic density should therefore taken with care.

Finally we emphasize that Ehrenfest based methods are not appropriate to treat the effects of high frequency intramolecular vibrations. When they are used in this regime, they invariably lead to unrealistically low mobilities, in contrast with the results of fully quantum treatments which predict only a moderate reduction of the mobility due to polaronic band renormalization (cf. Section 3.2).

4.3 Relaxation time approximation

The existence of a direct connection with the static disorder problem, that was anticipated in Sec. 4.1 and demonstrated by the Ehrenfest simulations (cf. Fig. 6(a)), suggests that despite the apparent band-like behavior of the mobility, the charge transport mechanism in organic semiconductors could be better understood by adopting a radically different paradigm, which takes localization as a starting point. A simple scheme to bridge between static and dynamical disorder has been developed in Refs. [52, 70, 92] based on a relaxation time approximation (RTA) applied to the localized limit. [104, 105] In addition to providing a very efficient method for the calculation of the mobility, which overcomes the drawbacks of the Ehrenfest method, the RTA scheme has the advantage of providing a transparent analytical insight on the microscopic mechanism of charge transport, clarifying both the relationship between mobility and localization and the crucial effects of molecular dynamics. Recently, it has been shown that the RTA becomes exact in a model for exciton transport where the inelastic scattering time is replaced by the decoherence time of the exciton. [106] The effects of short-time correlations in the dynamics of disorder have been recently studied in Ref. [107] using a stochastic model similar to Ref. [19].

Analytical insights on the transport mechanism: transient localization length and inelastic scattering time.– The idea underlying the RTA is to express the dynamical properties of the system under study in terms of those of a suitably defined reference system, from which it decays over time. [52, 92] As suggested from the preceding discussion, our reference system of choice will be an idealized version of the organic semiconductor where the molecular displacements are frozen. Such a reference system displays Anderson localization of the carriers. [12]

The key physical quantity for the RTA is the velocity *anticommutator* correlation function $C(t) = \{\hat{V}(t), \hat{V}(0)\}$, which is proportional to the time derivative of the instantaneous diffusivity, $C(t) = 2dD(t)/dt$ [52, 70, 92]. Taking for reference the velocity correlation function $C_0(t)$ of a system with static molecular displacements, we introduce the relaxation time approximation as follows: [3]

$$C_{RTA}(t) = C_0(t)e^{-t/\tau_{in}}. \tag{23}$$

It is clear from the above equation that the correlation function $C_{RTA}(t)$ coincides with that of the system with static disorder for $t \ll \tau_{in}$, because in this case $e^{-t/\tau_{in}} \simeq 1$. At longer times, however, the exponential term in Eq. (23) causes a decay of the velocity correlations. This decay physically corresponds to the destruction of the quantum interference processes that are at the origin of Anderson localization (the so-called backscattering terms), [109, 12] and that are encoded in the reference $C_0(t)$. According to the discussion in the previous Section, one should set τ_{in} of the order of the timescale of molecular motions, $1/\omega_0$. The spread $\Delta X^2_{RTA}(t)$ and instantaneous diffusivity $D_{RTA}(t)$ can be readily obtained via time integration of Eq. (23), and are illustrated in Fig. 6 (red thick lines). They exhibit the same qualitative behavior as seen in the Ehrenfest simulations, but do not suffer from the heating problem at long times.

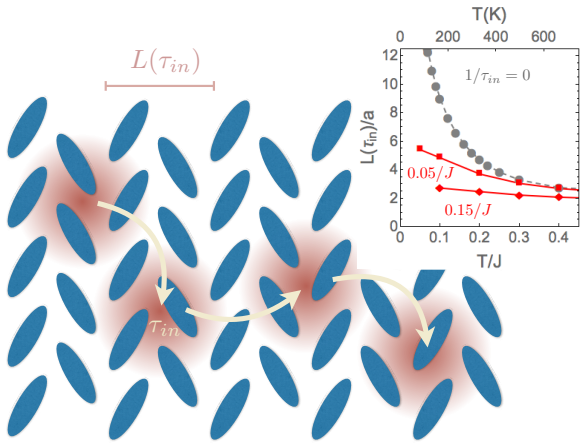

Figure 7: A sketch of the transport mechanism in the transient localization regime. The inset shows the temperature dependence of transient localization length $L(\tau_{in})$ of Eq. (24) for two different values of the inelastic scattering time.

From Eq. (23), the diffusion constant in the long time limit can be expressed as

$$D_{RTA} = \frac{L^2(\tau_{in})}{2\tau_{in}}. \tag{24}$$

Here $L^2(\tau_{in}) = \int e^{-t/\tau_{in}} \Delta X^2_0(t)dt/\tau_{in}$ is the electron spread achieved at a time $t \approx \tau_{in} \equiv 1/\omega_0$, just before diffusion sets back in (cf. Fig. 6). $L(\tau_{in})$ therefore has the meaning of a *transient localization length*. The slower the molecular motions, the closer it approaches the actual localization length L_0 of the reference system,

[3] Note that the standard description of semi-classical transport can be obtained by defining a reference C_0 corresponding to the opposite limit of a perfectly periodic crystal, and subsequently including the scattering of Bloch waves by phonons and impurities via an analogous exponential relaxation term. [108]

which is exactly attained in the limit where $\tau_{in} \to \infty$: $L(\tau_{in} \to \infty) = L_0$. The temperature dependence of both the static and transient localization length is illustrated in the inset of Fig. 7.

The expression Eq. (24) is analogous to the Thouless diffusivity of Anderson insulators. [109] It represents a physical process where localized electrons diffuse over a distance $L(\tau_{in})$ with a trial rate $1/\tau_{in}$, as pictorially illustrated in Fig. 7. The corresponding mobility can be obtained from the Einstein relation as

$$\mu_{RTA} = \frac{e}{k_B T} \frac{L^2(\tau_{in})}{2\tau_{in}}. \quad (25)$$

The mobility calculated via Eq. (25) by taking $\tau_{in}\omega_0 = 1$ and the microscopic parameters appropriate for rubrene is reported in Fig. 5 (red full line). Several remarks are in order:

(i) From Eq. (25) we can understand the origin of the "metallic-like" power-law behavior of the mobility in organic semiconductors, as arising both from the explicit $1/T$ factor and from the temperature dependence of the transient localization length $L(\tau_{in})$. The latter decreases with temperature because the carriers tend to be more and more localized upon increasing the thermal molecular disorder, as shown in the inset of Fig. 7. In the regime of parameters relevant to rubrene, the RTA results for the model Eq. (1) are well reproduced by the following functional form: [52]

$$L^2(\tau_{in}) \simeq a^2 \frac{c_{\tau_{in}}}{\lambda^l} \left(\frac{J}{T}\right)^q. \quad (26)$$

with a prefactor $c_{\tau_{in}}$ which depends weakly on τ_{in}. Fitting the numerical data for $1/\tau_{in} = 0.05J$ with the above form in the interval $0.14 < \lambda < 0.21$ and $0.18 < T/J < 0.3$ yields $l = 1.64 \pm 0.03$ and $q = 0.94 \pm 0.02$. Substituting this into Eq. (25) leads to a mobility varying as $\mu \propto T^{-p}$ with $p = 1 + q$, i.e. roughly

$$\mu \propto T^{-2} \quad (27)$$

(see Ref. [51] for similar arguments applied to the case of acoustic phonons).

(ii) The temperature dependence predicted above corresponds to a system kept at constant volume. It is known however that the lattice parameters in organic semiconductors change appreciably with temperature, which is accompanied by changes in the transfer integrals [49, 89, 90]. Obviously, such changes can also affect the behavior of the mobility.

(iii) As can be seen from the comparison of Figs. 3 and 5, the mobility in the presence of transient localization is considerably lower than that of semi-classical carriers (cf. also the instantaneous diffusivity of Fig. 6). It is then easy to understand that Eq. (25) can properly describe mobilities that, as in the experiments, fall below the so-called Mott-Ioffe-Regel limit (cf. Sec.3.1.2), which is where the apparent mean-free path falls below the typical inter-molecular distance a. We also understand from Eq. (25) why organic semiconductors are a particularly favorable ground for this breakdown to occur: the large thermal molecular disorder leads to short $L(\tau_{in})$ (which reduce to few lattice spacings at room temperature even in pure samples) and the large values of the molecular mass lead to a large τ_{in}, both effects contributing to produce low values of μ in Eq. (25). Fig. 5 illustrates that the Mott-Ioffe-Regel limit is indeed approached in pure samples around room temperature, both in the experimental and in the theoretical results.

(iv) It is clear from Fig. 6 that the transient localization phenomenon only occurs provided that the inelastic scattering time is longer than the time τ_b that characterizes the onset of localization, $\tau_{in} \gtrsim \tau_b$, or equivalently, $\omega_0 \lesssim \hbar/\tau_b$ (typical values of $\hbar/\tau_b$ range from few units to few tens of meV, see Sec. 4.5.2 and Ref. [70]). In the opposite regime, i.e. for sufficiently large values of ω_0, localization processes are completely washed out and semi-classical transport is recovered. Conversely, if the inter-molecular transfer integrals are too low or if the electron-vibration coupling is larger than a critical value $\lambda_c = 0.5$, the electronic wavefunction becomes self-trapped to essentially a single inter-molecular bond, $L \simeq a$, and one can expect the transport mechanism to become thermally activated.

(v) Finally, we mention that the RTA results for the mobility are very close to the results of both the Ehrenfest simulations and the fully quantum simulations of Ref. [102] (see Sec. 4.4). [4] The relatively modest computational cost of the RTA makes this method very interesting to numerically access large system sizes, [110] or to perform systematic screening studies of different compounds.

4.3.1 Strategies to improve the mobility

Beyond its numerical versatility, the analytical content of the RTA formula Eq. (25) can be used to make systematic predictions on how the mobility varies upon changing the microscopic parameters, in the regime where transient localization applies (i.e. for sufficiently large J, not too large ω_0 and not too large λ, in the sense specified in the preceding paragraphs). This can provide useful strategies to improve the performances of real compounds (a recent work describing different engineering strategies can be found in Ref. [111]). The following possibilities can be explored:

(i) Increasing the molecular overlaps, and therefore the transfer integral J. This could be achieved in principle by optimizing the crystal packing. Practical examples include chemical functionalization, the application of pressure, or strain [112] (in thin films or self-assembled monolayers). From the theoretical point of

[4] A detailed (unpublished) study of the take-off time of the quantum-spread in the Ehrenfest simulations suggests that these are closely described by the RTA if one sets $\tau_{in}\omega_0 = (0.5 \pm 0.1)$. Taking this value in Eq. (25) would slightly increase the mobility compared to what is shown in Fig. 5, improving further the agreement with the QMC results.

view, we observe that within the transient localization scenario there is no explicit dependence of the mobility on J, cf. Eq. (25). Variations of the transfer integrals will therefore only enter implicitly through the behavior of the transient localization length.

Using the analytical expression Eq. (26) valid in the regime $L \gtrsim a$ for the typical microscopic parameters that apply to rubrene, we obtain approximately

$$\mu \propto J^q \simeq J$$

at constant λ (because $q \simeq 1$). It has to be recognized, however, that any variation of the electron-vibration coupling strength λ induced by structural modifications will also add to the power-law dependence (see also point (ii) below). Although it is not possible to assess precisely how this parameter depends on the crystal structure without a detailed calculation, from the behavior depicted in Fig. 1 one can imagine two limiting situations:

Optimizing the $\pi-\pi$ distance. If the equilibrium perpendicular distance between the molecules is varied without changing the long-axis molecular displacement, then the relative slope of $J_{ij}(u_i-u_j)$ measured in units of the equilibrium J does not change. By definition, this amounts to keeping the parameter $\alpha = (1/J)(dJ/du)$ fixed, as can be directly checked from Eq. (1). In this case, from the expression $\lambda = \alpha^2(\hbar/2M\omega_0)(J/\hbar\omega_0)$ we see that λ *increases* proportionally to J, which yields for the mobility

$$\mu \propto J^{q-l} \simeq J^{-0.7}.$$

We conclude that, quite unexpectedly, a reduction of the perpendicular $(\pi-\pi)$ distance between neighboring molecules along a stack will be detrimental to the mobility.

Optimizing the long-axis distance. If instead the lateral coordinate is varied without changing the perpendicular distance, then the parameter α changes with J, and the coupling constant λ also changes accordingly. Adopting a linear approximation for $J_{ij}(u_i-u_j)$, which is generally valid far from the extrema of the curve in Fig. 1, one has in this case $\alpha = (1/J)(dJ/du) \propto 1/J$. Consequently for long-axis displacements the coupling decreases upon increasing the transfer integral as $\lambda \propto 1/J$, which adds up to give

$$\mu \propto J^{q+l} \simeq J^{2.6}.$$

Note that if the equilibrium displacements $u_i - u_j$ in a given material are already close to the extrema (as is the case for rubrene, cf. Fig. 1) neither J nor λ depend much on the equilibrium displacement $u_i - u_j$, so that optimizing the structure will not lead to major improvements of the mobility.

The three contradictory behaviors identified above imply that it is difficult to identify a general rule predicting how the mobility depends on the inter-molecular transfer integrals, and case by case structural calculations are needed. This might explain why recent studies on crystals of functionalized rubrene molecules [113] could not identify a clear trend relating μ and J.

(ii) Reducing the coupling with the inter-molecular motions, which results in an increase of the transient localization length. The discussion at point (i) indicates that this can be achieved by adjusting the crystal packing to minimize the dependence of the inter-molecular transfer with inter-molecular distance, i.e. the slope of $J_{ij}(u_i - u_j)$, which is essentially the parameter α of Eq. (1). Accounting for the dependence of the transient localization length Eq. (26) on the coupling constant yields

$$\mu \propto \lambda^{-l} \propto \alpha^{-2l},$$

with $l \simeq 1.64$.

(iii) Increasing the inter-molecular vibration frequency ω_0 by tightening the inter-molecular bonds. The frequency of inter-molecular vibrations enters explicitly in the formula Eq. (25) for the mobility: varying ω_0 while keeping λ and J fixed should affect the mobility linearly, because $1/\tau_{in} \propto \omega_0$. The numerical results of [52] show that the effect is actually sub-linear, $\mu \propto \omega_0^{\zeta}$, with $\zeta \simeq 0.35$ for small variations around $\omega_0/J = 0.05$. This weaker power law can be ascribed to the appreciable dependence of $L(\tau_{in})$ on τ_{in}: the transient localization length diminishes when τ_{in} decreases, i.e. when the frequency of the molecular motions increases, cf. Figs. 6 and 8.

To assess the overall effect of an increase of ω_0 on the mobility, one has again to account for the explicit dependence of the coupling to inter-molecular motions. The coupling constant strongly decreases as $\lambda \propto 1/\omega_0^2$, which leads to a total

$$\mu \propto \omega_0^{2l+\zeta} \simeq \omega_0^{3.6}.$$

Tightening the inter-molecular bonds therefore appears as a very efficient strategy to increase the mobility in organic semiconductors. This could be achieved for example by functionalizing the molecules with rigidly bound side groups, which would confine the long-axis displacements of the molecules, effectively increasing ω_0. Similarly, it is expected that smaller molecules will have less ease in sliding along the long axis, also leading to generally larger vibrational frequencies. We note that for sufficiently large values of ω_0, eventually a semi-classical transport mechanism should recovered, again leading to appreciably higher values of the mobility as illustrated in Fig. 3 (see the discussion at point (iv) in Sec. 4.3).

We note that changing the molecular mass M (as in an isotope substitution experiment) does not affect the electron-vibration coupling constant λ. This can be directly checked from the expression of λ given above, and noting that $\omega_0 = \sqrt{K/M}$ with K the force constant. As a result, the effect of mass substitutions on the mobility would be weak.

4.4 Other quantum approaches

Surface hopping methods.– In the original Eherenfest method, the oscillators evolve along a single, *averaged* potential. The surface-hopping method developed by Tully [114] is a dynamical procedure which modifies Ehrenfest's equations of motion for classical oscillators to include the switching from one adiabatic surface to another, which is valid under the assumption that electronic coherence is lost in a time shorter than the average surface hopping time. This allows to take into account correlations between the lattice displacements and the electron density, giving access to processes close to the small polaron incoherent hopping regime (the Ehrenfest method can, on the contrary, be considered too coherent and the chemical physics literature contains methods to reduce its coherence time [115]).

A Flexible Surface Hopping scheme was devised in Ref. [45] in order to treat large systems, where only a relevant fraction of the original system is treated with surface hopping with a proper choice of the time-step. The method was applied to a model Hamiltonian similar to that of Eq. (1) which includes also a coupling to intramolecular vibrations. The resulting mobilities show a power law behavior in the region of interest provided that the coupling with intramolecular vibrations is not too strong. In the opposite regime of strong coupling with the intramolecular vibrations, instead, the correlation between the lattice distortions and the denisty gives rise to small polaron formation, in which case a hopping transport regime is achieved. At intermediate coupling strengths a coexistence of localized and delocalized charges is found with this method, in agreement with the equilibrium Green's function calculations of Ref. [62].

Lorentzian broadening of the optical conductivity in the static disorder problem.– The mobility of a system can in principle be obtained from the knowledge of the frequency dependent conductivity. This is given by the Kubo formula, [75] which can be stated as

$$\sigma(\omega) = \frac{1}{\nu\hbar\omega} Re C_{-}^{R}(\omega), \tag{28}$$

where $C_{-}^{R}(\omega)$ is the Fourier transform of the current-current *commutator* correlation function. The mobility can then be calculated from the zero-frequency limit of the above expression as [75]

$$\mu = \lim_{\omega\to 0^+} \frac{1}{e k_B T \frac{\partial n}{\partial \mu}} Re\ \sigma(\omega) \tag{29}$$

where n is the carrier density. At low density, the denominator of Eq. (29) reduces to (en) and one obtains $\sigma_{dc} = ne\mu$.

An approximation method alternative to the RTA presented above has been used in Ref. [116] to evaluate the carrier mobility starting from the static disorder problem. Using the Lehman representation for $ReC_{-}^{R}(\omega)$ in terms of the eigenstates $|n\rangle, |m\rangle$ of the *static* Hamiltonian ($\omega_0 \to 0$) gives

$$Re\ \sigma(\omega) = \frac{2\pi e^2}{\nu\hbar\omega} \sum_{n,m} e^{-\beta E_n} \times \tag{30}$$
$$|\langle n|\hat{J}|m\rangle|^2 \times (f(E_n) - f(E_m))\delta(\omega - E_m + E_n)$$

where $\hat{J}$ is current operator and $f(E)$ is the Fermi function. The above expression implies that $\sigma_{dc} = \sigma(\omega \to 0) = 0$, and therefore $\mu = 0$. A finite mobility can be obtained by introducing a lorentzian broadening in the delta functions appearing in Eq. (30).

The results obtained by this method are numerically very close to the RTA (see the data labeled "conv. σ" in Fig. 5, obtained with a broadening = $\hbar\omega_0$). This happens because allowing for a finite broadening in the calculation of $C_{-}^{R}(\omega)$ is mathematically similar to the RTA scheme of Sec. 4.3, where a finite inelastic scattering time was introduced at the level of the *anticommutator* current-current correlation function. [52] However, the *physical content* of the theory is different. In Ref. [116] the broadening was assumed to originate from the quantum zero-point motion of the molecular vibrations. This should be contrasted with the RTA equations of Sec. 4.3, which show that inelastic scattering processes associated with the molecular fluctuations are sufficient to provide a finite mobility already when the molecular vibrations are classical, $k_B T > \hbar\omega_0$.

QMC with analytical continuation.– Recently, a Quantum Monte Carlo (QMC) approach has been applied to the study of the model Eq. (1) by De Filippis *et al.* [102] The authors combine diagrammatic [117] and worldline Monte Carlo approaches to evaluate the conductivity on the imaginary time axis. An analitycal continuation scheme is then used to obtain the complex optical conductivity on the real axis [118] with the aid of exact diagonalization of a small cluster. This constitutes at present the most complete treatment of quantum effects, and it is in principle unbiased.

The results of this procedure, reported in Fig. 5, fall very close to the RTA, Ehrenfest and convolution methods presented above (we have rescaled the data of Ref. [102] to the value of the transfer integral $J = 143meV$ for comparison with the other methods). Using the formalism presented in Sec. 4.5, the authors also calculate the instantaneous diffusivity, and find a subdiffusive behavior of the system at room temperature, in agreement with the transient localization scenario.

We note that as was done in Ref. [70] (see next Section), Ref. [102] proposes a phenomenological modeling of the optical absorption data. De Filippis *et al.* interpretation of the numerical results is based on the assumption that a large polaron is formed due to the correlation between the carrier and the induced molecular deformation, i.e. self-trapping. The finite-frequency absorption would then be caused by the internal degrees of freedom

of such polaronic particle (which supposedly exists already at $T = 0$), not by the thermal molecular motions (which instead dominate at room temperature). Accordingly, the authors of Ref. [102] fit the numerical data based on the Drude-Lorentz model, which highlights the existence of an electronic bound state with a finite radius.

The whole interpretation in Ref. [102] therefore relies on the existence of large-polaron correlations. In the considered model Eq. (1) and at the values of λ characteristic of organic semiconductors, however, the electron is completely free in the adiabatic regime [64, 94, 119] and the large-polaron correlations present at finite values of the phonon frequency are unlikely to survive the thermal lattice fluctuations at room temperature. A phenomenological model based on the localization induced by thermal molecular motions, and which does not require the presence of polaronic electron-lattice correlations, is presented in Sec. 4.5.2 below. [70]

4.5 Optical conductivity

4.5.1 Exact relationships

An expression was derived in Ref. [92] which identifies the quantum spread $\Delta X^2(t)$ in the time domain as the physical quantity that is dual to the optical conductivity $\sigma(\omega)$ in the frequency domain:

$$\sigma(\omega) = -ne^2\omega^2 \frac{\tanh(\beta\hbar\omega/2)}{\hbar\omega} Re \int_0^\infty e^{i\omega t} \Delta X^2(t) dt, \tag{31}$$

with $\beta = 1/k_B T$ and n the electron density. This relation, which is a restatement of the Kubo response function theory [75] based on the formal developments by Mayou and collaborators [104, 105], is *exact* for non-degenerate semiconductors. It can be inverted to give

$$\Delta X^2(t) = -\frac{2\hbar}{\pi e^2} Re \int_0^\infty e^{-i\omega t} \frac{\sigma(\omega)/n}{\omega \tanh(\beta\hbar\omega/2)} d\omega. \tag{32}$$

This pair of equations shows that the quantum spread of the carriers' wavefunctions and the optical response are deeply interconnected physical quantities. Eq. (31) can be used to obtain the optical conductivity $\sigma(\omega)$ from the theoretical knowledge of the time-dependent quantum spread $\Delta X^2(t)$, i.e. precisely the quantity that is at the core of both the Ehrenfest and the RTA treatments presented above. For example, via the RTA equations of Sec. 4.3, one can easily calculate the optical conductivity in the presence of dynamical molecular motions from the knowledge of $\sigma(\omega)$ in the limit of static displacements, as was done in Ref. [92].

Conversely, Eq. (32) allows to infer the time-dependent quantum dynamics of charge carriers from the calculated [92, 102] or measured [92] optical absorption in an organic semiconductor. Eq. (32) therefore implies that optical absorption measurements are able to provide fundamental information on the transport mechanism, that are complementary to the analysis of the temperature dependence of the mobility [52, 70, 92]. In particular, the existence of an intermediate regime of localization between the ballistic evolution at short times and the diffusion at long times (cf. Fig. 6) translates, through Eq. (32), into a characteristic "Drude-Anderson" optical absorption shape [70], which exhibits a finite frequency peak related to the transient localization of the carriers (see next paragraph). The direct observation of such a finite-frequency peak in the optical absorption measurements performed on rubrene single crystals [38, 37, 24] (cf. Sec. 2.1 and the experimental data in Fig. 9) therefore provides a strong and direct evidence supporting the transient localization phenomenon.

4.5.2 A phenomenological model for the analysis of experiments

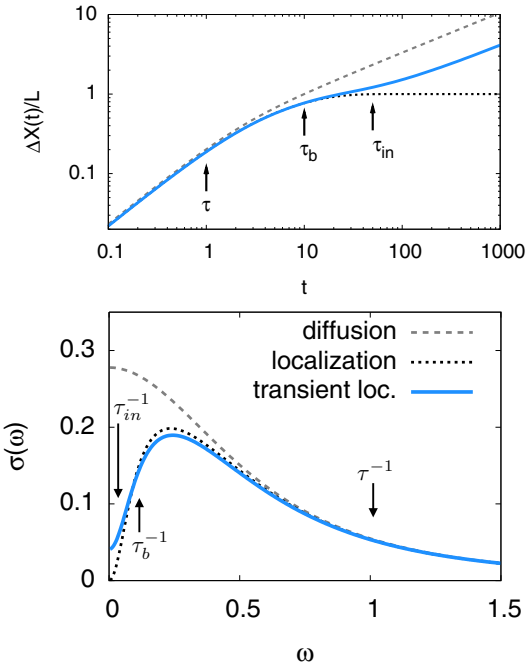

Figure 8: Time dependent quantum spread (top) and optical conductivity (bottom) in the phenomenological model described by Eqs. (33) and (34). The arrows indicate the different timescales of the model, here taken as $\tau = 1$ (chosen as the time unit; frequencies are in units of $1/\tau$), $\tau_b = 10$, $\tau_{in} = 50$, and $k_B T = 0.2\hbar/\tau$. In both panels, the black dotted line is the localized limit, obtained for $\tau_{in} \to \infty$. The gray dashed line is the Drude-like diffusive response alone, corresponding to the first term in Eq. (34). Reprinted from Ref. [70].

We have presented in Sec. 4.3 the RTA as a powerful and efficient method to bridge between the limit of static disorder and the case of dynamical molecular motions appropriate to organic semiconductors, and shown that it provides results for the mobility that are in good quantitative agreement with the most accurate methods available to date. As was pointed out above, however, the

greatest success of the RTA scheme is that it provides a transparent picture of the charge transport mechanism, showing in simple terms how the incipient carrier localization and the dynamics of the molecular motions enter into play.

The analytical insights developed in Sec. 4.3 can actually be pushed one step forward, and used to extract the relevant microscopic parameters of charge transport directly from the experimental optical absorption data. To this aim, a phenomenological model was developed in Ref. [70] which provides an analytical ansatz to the reference correlation function $C_0(t)$ in Eq. (23), so that no numerical calculations are needed throughout the analysis. The model is defined in terms of few relevant microscopic parameters already introduced above: these are the carrier localization length L_0, the elastic scattering time τ, and the backscattering time $\tau_b > \tau$ encoding the characteristic timescale of the localization process. The correlation function is written as the difference between two exponentials, the first representing semi-classical scattering, the second being the backscattering term:

$$C_0(t) = \frac{L_0^2}{\tau_b - \tau}\left(\frac{1}{\tau}e^{-t/\tau} - \frac{1}{\tau_b}e^{-t/\tau_b}\right). \qquad (33)$$

The inelastic scattering time τ_{in} representing the dynamics of disorder is included via Eq. (23). The corresponding time dependent quantum spread is illustrated in Fig. 8 (top), and correctly reproduces the qualitative features of the simulations shown in Fig. 6. With this set of parameters, the mobility takes the RTA form $\mu = (e/k_BT)L^2(\tau_{in})/(2\tau_{in})$ [cf. Eq. (25)]. The transient localization length is given by $L^2(\tau_{in}) = L_0^2/(1 + \tau/\tau_{in})(1 + \tau_b/\tau_{in})$, which properly tends to the static localization length L_0 when $\tau_{in} \to \infty$.

The corresponding optical conductivity is obtained in analytical form as: [70]

$$Re\ \sigma(\omega) = \frac{ne^2L_0^2}{\tau_b - \tau}\frac{\tanh(\frac{\hbar\omega}{2k_BT})}{\hbar\omega} \times \qquad (34)$$
$$\times Re\left[\frac{1}{1 + \tau/\tau_{in} - i\omega\tau} - \frac{1}{1 + \tau_b/\tau_{in} - i\omega\tau_b}\right].$$

Together with the real (dissipative) part, we also report here for the first time the imaginary (refractive) part, that is obtained through a Kramers-Krönig transformation. It can be expressed via a rapidly converging sum over fermionic Matsubara frequencies $\omega_m = (2m + 1)\pi T$ as follows:

$$Im\ \sigma(\omega) = \frac{ne^2L_0^2}{\tau_b - \tau}4k_BT\sum_{m=0}^{\infty}\frac{1}{\omega_m}\frac{\omega}{\omega^2 + \omega_m^2} \times \qquad (35)$$
$$\times\left[\frac{1}{1 + \tau/\tau_{in} + \omega_m\tau} - \frac{1}{1 + \tau_b/\tau_{in} + \omega_m\tau_b}\right].$$

The above Eqs. (34) and (36) can also be generalized to the case of degenerate electron systems (see Ref. [70] and Sec. 4.6 below).

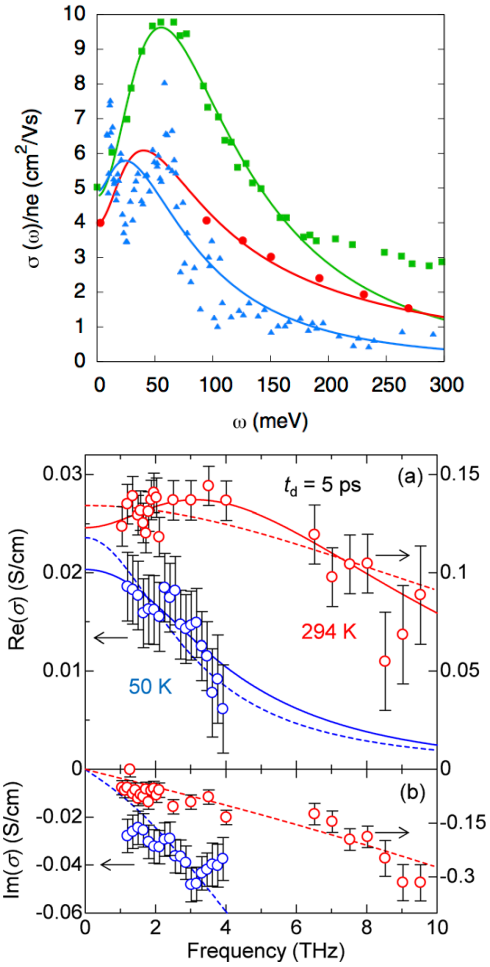

Figure 9: Top: Optical conductivity measured in rubrene FETs. The full lines are fits through Eq. (34) from Ref. [70]; the data are from Refs. [37] (triangles) [38] (squares) and [120] (circles). Bottom: real and imaginary parts of $\sigma(\omega)$ measured after photoexcitation in Ref. [24]. The full line is Eq. (34), which properly captures the maximum in the room temperature data, while dashed lines are Drude fits.

The present analytical expressions have been proven to be quite accurate to describe the region of the Drude-Anderson peak in the optical conductivity of the model Eq. (1), [70] because localization phenomena occur in a frequency range where the details of the band dispersion are not important: band effects, that are not contained in the analytical ansatz for C_0, only appear at much higher frequencies $\omega \sim J$ where the carrier absorption progressively vanishes anyway.

Both Eqs. (34) and (36) can be easily implemented in a fitting procedure. For example, applying the above Eq. (34) to fit the measurements of Ref. [38] nicely reproduces the shape of the experimental peak (green squares in the top panel of Fig. 9), and yields the following parameters: $\hbar/\tau_{in} = 13meV$, $\hbar/\tau_b = 40meV$, $\hbar/\tau = 195meV$ and $L_0/a = 1.9$. The extracted inelastic scattering rate $\hbar/\tau_{in}$ is consistent with the frequency of

the intermolecular vibrations in rubrene, $\omega_0 = 5-15meV$ (cf. Sec. 2.3); the elastic scattering rate is of the same order of magnitude as the quasi-particle scattering rates commonly measured in ARPES measurements in organic semiconductors (see e.g. [88]); the extracted transient localization length indicates that the hole carriers are delocalized over few molecules, in agreement with other experimental probes (cf. Sec. 2.1) and with the theoretical results of Fig. 7.

A similar analysis was performed in Ref. [24] on pump-probe optical conductivity measurements in rubrene. The analysis of the room temperature data, shown in the bottom panel of Fig. 9, yields $\hbar/\tau_{in} = 8.9meV$ (again in the correct range of the molecular vibrations), $\hbar/\tau_b = 3.4meV$ and $\hbar/\tau = 34meV$. The backscattering rate inferred from the position of the peak, $\omega \approx 4THz \sim 12meV$, is much lower than that observed in rubrene FETs, indicating a reduced level of extrinsic disorder due to the bulk nature of the pump-probe measurement. This is also confirmed by the evolution of the spectrum with temperature: if extrinsic disorder was dominant, the backscattering rate would increase at low temperatures [70]; instead, the fit at $T = 50K$ yields a reduced value $\hbar/\tau_b = 2.7meV$, demonstrating that the pump-probe measurements are free from interface effects and are actually probing the intrinsic carrier dynamics in the organic semiconductors.

4.6 Degenerate systems

Although in this overview we have mainly focused on the transient localization phenomenon in organic semiconductors, the concept itself is much more general and applies as well to other classes of materials.

The interplay between Anderson localization and lattice vibrations was studied in the past in the different framework of random metal alloys and other degenerate disordered systems. It was recognized early on by Gogolin and collaborators [121, 122] and Thouless [109] that the random fluctuations introduced by the lattice motions destroy the quantum interferences necessary for localization of the electronic states, which is precisely the idea underlying the RTA treatment presented in Sec. 4.3. In the scaling theories of localization, [12] the inelastic scattering by dynamical lattice motions is included as a cutoff for localization corrections, allowing an otherwise localized electron system to support a finite electrical conductivity. Beyond such scaling arguments, a microscopic calculation of the effects of lattice dynamics on charge transport in strongly disordered systems based on the Kubo formula was provided by Girvin and Jonson. [123]

The case of one-dimensional disordered systems was studied in depth by several authors via diagrammatic techniques [122, 124, 125, 126]. These authors provided an estimate for the diffusivity equivalent to Eq. (24),

$$D \sim \frac{L^2}{\tau_{in}}. \tag{36}$$

A physical interpretation of this formula was given in terms of electrons being localized at intermediate time-scales by the dynamic disorder introduced by the phonons, which is in essence equivalent to the transient localization mechanism discussed in this review. The concept was also generalized to 2D systems in Refs. [127, 128].

Interestingly, these ideas were actually applied [122, 129, 126] to the analysis of the transport and optical properties of both one- and two-dimensional organic conductors, taking the compound TTF-TCNQ as a paradigmatic case. Low-dimensional organic conductors can be viewed as the doped (degenerate) analogues of the organic semiconductors discussed in this overview. In particular, they have narrow bands constructed from the pi-overlaps between adjacent organic molecules, and therefore the effects of inter-molecular motions should be analogous to those in organic semiconductors. Although in such degenerate electron systems collective effects related to electron correlations can enter into play at low temperatures [129, 130, 133, 134], the effects of thermal lattice motions should become dominant at high temperatures, and it is not suprising that also in this class of materials several distinctive features of the transient localization mechanism are commonly observed: metallic-like power-law temperature dependence of the conductivity, with low values $\sigma = 10 - 1000(\Omega cm)^{-1}$ [135] corresponding to room temperature mobilities in the range $\mu = 0.1 - 10cm^2/Vs$; breakdown of the MIR condition; apparent localization lengths of few molecular units; and non-Drude-like optical conductivities exhibiting marked finite-frequency peaks in the infra-red region [130, 131] (see [70] for a detailed discussion).

It would be interesting to apply the full phenomenological model of Sec. 4.5.2 to perform a systematic analysis of the experimental results in low-dimensional organic conductors [136] and other classes of compounds. To this aim we report here the formulas which generalize Eqs. (34) and (36) to degenerate electron systems in the low temperature limit: [70]

$$\sigma(E_F,\omega) = e^2 N(E_F) \frac{C(E_F,0)}{1/\tau - 1/\tau_b} \times \\ \times \left[\frac{1}{1+\tau/\tau_{in} - i\omega\tau} - \frac{1}{1+\tau_b/\tau_{in} - i\omega\tau_b} \right] \tag{37}$$

with $N(E_F)$ the density of states at the Fermi energy and $C(E_F,0)$ the short-time limit of the velocity correlation function of electrons at the Fermi energy. We conclude this section with some remarks.

(i) The above formula has been used in Ref. [70] to fit the room temperature optical conductivity data in the two-dimensional compound θ-ET_2I_3 [130] (a compound where $\sigma = 10(\Omega cm)^{-1}$ at room temperature, below the Mott-Ioffe-Regel limit [73]). A backscattering rate $\hbar/\tau_b \simeq 14meV$ could be extracted, as well as an elastic scattering rate $\hbar/\tau = 116meV$, both in the correct range expected from electron-molecular vibration

coupling. An analogous absorption peak in the far infrared range has also been observed in the compound θ-ET_2CsZn, which presents a glassy electronic state. [131] In that case, in addition to the dynamical molecular disorder, the effect of the random electrostatic potentials of the electrons in the glassy configurations [132] could also give rise to an absorption shape of the form of Eq. (37).

(ii) Ideally, the realization of FETs with ionic liquid gating can bridge continuously from the physics of non-degenerate organic semiconductors to that of degenerate organic conductors. It has been shown recently in Ref. [137] that in rubrene, carrier densities up to $6\times10^{13}cm^{-2}$ can be reached by this technique (0.3 holes per molecule), where not only the Fermi-Dirac statistics but also many-body electron correlation effects become important. It would be extremely interesting to track the evolution of the electronic properties as a function of carrier concentration in such devices.

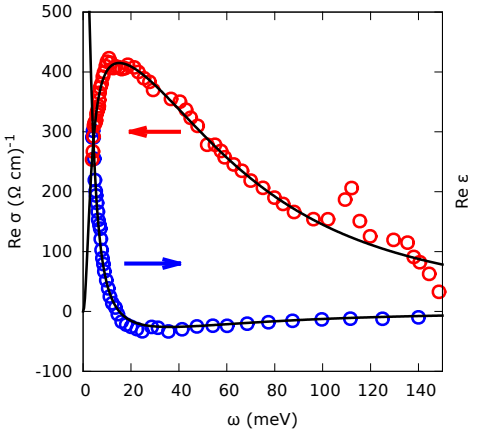

Figure 10: Real part of the optical conductivity Reσ and dielectric constant $Re\ \varepsilon = 1 - 4\pi \mathrm{Im}\sigma/\omega$ (in arb. units) measured in carbon nanotubes, simultaneously fitted through Eq. (37). Data are from Ref. [138].

(iii) In a different class of low-dimensional materials — carbon nanotubes — an ubiquitous optical absorption peak in the far infrared range has been reported by several groups [138, 139, 140], whose microscopic origin could possibly be related to the transient localization phenomena described in this work. Fig. 10 illustrates the (simultaneous) fits of both the real and imaginary part of the optical conductivity measured in Ref. [138] via Eq. (37), showing an excellent agreement with the data. The extracted values are $\hbar/\tau_b \simeq 3.3meV$ and $\hbar/\tau = 68meV$ ($\tau_{in} \gg \tau_b, \tau$ was assumed).

5 Outlook

Understanding the intrinsic charge transport mechanism in high-mobility organic semiconductors requires a theory that is able to reconcile the apparent contradiction between the "band-like" temperature dependence of the mobility, suggestive of the existence of extended charge carriers, and the presence of localization phenomena as seen in a variety of experiments. It is now ascertained that such duality originates, at the microscopic level, from the presence of large thermal molecular motions. Dynamical deviations from the perfect crystalline arrangement act as a strong source of disorder, inducing a localization of the electronic wave functions on the typical timescales of the inter-molecular vibrations. Such *transient localization* is what limits the room temperature mobilities down to few tens of cm^2/Vs, as observed in the best organic semiconductors.

In this article, we have provided an overview of the different theoretical approaches that have been applied to the problem, focusing on an extensively studied model, Eq. (1), which describes the interaction of the charge carriers with the inter-molecular motions. The standard treatments based either on semi-classical band transport or polaron hopping, presented in Sec. 3, have been shown to be unable to provide a satisfactory description of the experiments, because they cannot capture the quantum localization effects caused by the large molecular motions. The corresponding results for the temperature dependence of the mobility are summarized in Fig. 3: while a band-like power-law dependence is commonly obtained, these methods generally overestimate the absolute value of the mobility, in the worst cases by a full order of magnitude.

Sec. 4 describes a number of theoretical approaches that have been developed recently and that can properly account for the effects of strong dynamical disorder. All these methods, which give direct access to the time evolution of the electronic wavefunction, indicate that the carriers become localized up to timescales corresponding to the period of the molecular oscillations. Such transient localization results in an original regime of charge transport where the carriers exhibit both localized and extended characters, as observed in experiments.

Sec. 4 also contains a description of some important analytical developments which help shed light on the microscopic transport mechanism at work in organic semiconductors. First, by taking quantum localization effects as a starting point, the relaxation time approximation described in Sec. 4.3 allows to understand in simple physical terms how the transient localization caused by dynamical molecular motions relates to the Anderson localization realized for static disorder. Next, the general theoretical framework presented in Sec. 4.5 identifies the optical conductivity in the frequency domain as a physical quantity that provides crucial information on the charge transport mechanism, complementary to the temperature dependence of the mobility. In particular, it is shown that the transient localization phenomenon is directly reflected in the emergence of a finite-frequency peak in the optical conductivity, whose existence in organic semiconductors has been confirmed experimentally by different groups.

In the regime of microscopic parameters appropriate to high mobility organic semiconductors, all the modern theoretical approaches presented in Sec. 4 yield quanti-

tatively comparable results for the temperature dependence and absolute value of the charge carrier mobility. As shown in Fig. 5, a remarkable agreement is found with the experimental data available in rubrene FETs, especially considering the simplicity of the model Eq. (1). With the limitations described in Sec. 2 in mind, the calculations presented in Sec. 4 thus have a real predictive power. Moreover, having identified how the different microscopic parameters enter in the charge transport processes allows one to devise efficient strategies to improve the performances of actual organic devices. According to Fig. 5, for example, if all sources of extrinsic disorder were removed one could attain mobilities above $100 cm^2/Vs$ upon lowering the temperature below $100K$. From the analytical arguments given in Sec. 4.3, seeking compounds with tighter inter-molecular bonds in order to reduce the inter-molecular fluctuations appears as a promising route to improve the transport characteristics of organic semiconductors.

Finally, it appears the general phenomenon of transient localization, discussed here in the framework of the crystalline organic semiconductors, is actually relevant in broader classes of materials such as low-dimensional organic metals, as well as glassy and disordered systems. A similar concept of environment-assisted quantum transport has also been put forward to explain charge transfer in biological light-harvesting systems [141, 142, 143].

References

[1] J.-L. Brédas, D. Beljonne, V. Coropceanu, J. Cornil, *Chem. Rev.*, **2004**, 104, 4971.

[2] J.-L. Brédas, J. E. Norton, J. Cornil, V. Coropceanu, *Accounts Chem. Res.*, **2009**, 42, 1691.

[3] N. A. Minder, S. Ono, Z. Chen, A. Facchetti, A. F. Morpurgo, *Adv. Mater.*, **2012**, 24, 503.

[4] T. Sakanoue, H. Sirringhaus, *Nat. Mater*, **2010**, 9, 736.

[5] C. B. Duke, L. B. Schein. *Phys. Today*, **1980**, 33, 42.

[6] A. Devos, M. Lannoo. *Phys. Rev. B*, **1998**, 58, 8236.

[7] V. Coropceanu, M. Malagoli, D. A. da Silva Filho, N. E. Gruhn, T. G. Bill, J. L. Brédas. *Phys. Rev. Lett.*, **2002**, 89, 275503.

[8] C. Faber, J. Laflamme Janssen, M. Côté, E. Runge, X. Blase. *Phys. Rev. B*, **2011**, 84, 155104.

[9] A. Girlando, L. Grisanti, M. Masino, I. Bilotti, A. Brillante, R. G. Della Valle, E. Venuti. *Phys. Rev. B*, **2010**, 82, 035208.

[10] J. Sinova, J. Schliemann, A. S. Núñez, A. H. MacDonald, *Phys. Rev. Lett.*, **2001**, 87, 226802.

[11] A. Troisi, G. Orlandi, *Phys. Rev. Lett.*, **2006**, 96, 086601.

[12] P. A. Lee, T. V. Ramakrishnan. *Rev. Mod. Phys.*, **1985**, 57, 287.

[13] H. Bässler, *phys. status solidi (b)*, **1993**, 175, 15.

[14] R. Coehoorn, W. F. Pasveer, P. A. Bobbert, M. A. J. Michels. *Phys. Rev. B*, **2005**, 72, 155206.

[15] I.I. Fishchuk, V. I. Arkhipov, A. Kadashchuk, P. Heremans, H. Bässler *Phys. Rev. B*, **2007**, 76, 045210.

[16] S. H. Glarum, *J. Phys. Chem. Solids*, **1963**, 24, 1577.

[17] L. Friedman, *Phys. Rev.*, **1965**, 140, A1649.

[18] P. Gosar and Sang-il Choi. *Phys. Rev.*, **Oct 1966**, 150:529–538.

[19] A. Madhukar and W. Post. *Phys. Rev. Lett.*, **Nov 1977**, 39:1424–1427.

[20] H. A. v. Laarhoven, C. F. J. Flipse, M. Koeberg, M. Bonn, E. Hendry, G. Orlandi, O. D. Jurchescu, T. T. M. Palstra, A. Troisi, *J. of Chem. Phys.*, **2008**, 129, 044704.

[21] H. Sirringhaus, T. Sakanoue, J.-F. Chang, *phys. status solidi (b)*, **2012**, 249, 1655.

[22] J.-F. Chang, T. Sakanoue, Y. Olivier, T. Uemura, M.-B. Dufourg-Madec, S. G. Yeates, J. Cornil, J. Takeya, A. Troisi, H. Sirringhaus, *Phys. Rev. Lett.*, **2011**, 107, 066601.

[23] A. S. Eggeman, S. Illig, A. Troisi, H. Sirringhaus, P. A. Midgley, *Nat. Mater.*, **2013**, 12, 1045.

[24] H. Yada, R. Uchida, H. Sekine, T. Terashige, S. Tao, Y. Matsui, N. Kida, S. Fratini, S. Ciuchi, Y. Okada, T. Uemura, J. Takeya, and H. Okamoto, *Appl. Phys. Lett.*, **2014**, 105, 143302.

[25] N. A. Minder, S. Lu, S. Fratini, S. Ciuchi, A. Facchetti, A. F. Morpurgo, *Adv. Mater.*, **2014**, 26, 1254.

[26] D. L. Cheung, A. Troisi, *Phys. Chem. Chem. Phys.*, **2008**, 10, 5941.

[27] A. Troisi, *Chem. Soc. Rev.*, **2011**, 40, 2347.

[28] V. Coropceanu, J. Cornil, D. A. da Silva Filho, Y. Olivier, R. Silbey, J.-L. Brédas, *Chem. Rev.*, **2007**, 107, 926.

[29] G. Schweicher, Y. Olivier, V. Lemaur, Y. H. Geerts, *Israel J. Chem.*, **2014**, 54, 595.

[30] *Organic Electronics II* (Ed. Hagen Klauk), Wiley-VCH Verlag Gmbh & Co. KGaA, **2012**.

[31] Z. Shuai, L. Wang, Q. Li, *Adv. Mater.*, **2011**, 23, 1145.

[32] S. Stafstrom, *Chem. Soc. Rev.*, **2010**, 39, 2484.

[33] K. P. Pernstich, B. Rossner, B. Batlogg. *Nat. Mater.*, **2008**, 7, 321.

[34] V. Podzorov, E. Menard, J.A. Rogers, M.E. Gershenson, *Phys. Rev. Lett.*, **2005**, 95, 226601.

[35] W. L. Kalb, S. Haas, C. Krellner, T. Mathis, B. Batlogg, *Phys. Rev. B*, **2010**, 81, 155315.

[36] K. Willa, R. Häusermann, T. Mathis, A. Facchetti, Z. Chen, B. Batlogg, *J. Appl. Phys.*, **2013**, 113, 133707.

[37] M. Fischer, M. Dressel, B. Gompf, A. K. Tripathi, J. Pflaum, *Appl. Phys. Lett.*, **2006**, 89, 182103.

[38] Z. Q. Li, V. Podzorov, N. Sai, M. C. Martin, M. E. Gershenson, M. Di Ventra, D. N. Basov, *Phys. Rev. Lett.*, **2007**, 99, 016403.

[39] K. Marumoto, S.-I. Kuroda, T. Takenobu, Y. Iwasa, *Phys. Rev. Lett.*, **2006**, 97, 256603.

[40] H. Matsui, A. S. Mishchenko, T. Hasegawa, *Phys. Rev. Lett.*, **2010**, 104, 056602.

[41] K. Marumoto, N. Arai, H. Goto, M. Kijima, K. Murakami, Y. Tominari, J. Takeya, Y. Shimoi, H. Tanaka, S.-I. Kuroda, T. Kaji, T. Nishikawa, T. Takenobu, Y. Iwasa, *Phys. Rev. B*, **2011**, 83, 075302.

[42] a) T. Holstein, *Annals of Physics*, **1959**, 8, 325; b) T. Holstein, *Annals of Physics*, **1959**, 8, 343.

[43] M. Capone, S. Ciuchi, C. Grimaldi, *Europhys. Lett.*, **1998**, 42, 523.

[44] S. Fratini, S. Ciuchi, *Phys. Rev. Lett.*, **2003**, 91, 256403.

[45] L. Wang, D. Beljonne, *J. Phys. Chem. Lett.*, **2013**, 4, 1888.

[46] S. Mishchenko, A. N. Nagaosa, G. De Filippis, A. de Candia, V. Cataudella, *Phys. Rev. Lett.*, **2015**, 114, 146401.

[47] N Vukmirović, C. Bruder, V. M. Stojanović, *Phys. Rev. Lett.*, **2012**, 109, 126407.

[48] S. Ciuchi, S. Fratini, *Phys. Rev. Lett.*, **2011**, 106, 166403.

[49] S. Ciuchi, R. C. Hatch, H. Höchst, C. Faber, X. Blase, S. Fratini, *Phys. Rev. Lett.*, **2012**, 108, 256401.

[50] M. N. Bussac, J. D. Picon, L. Zuppiroli, *Europhys. Lett.*, **2004**, 66, 392.

[51] J.-D. Picon, M. N. Bussac, L. Zuppiroli, *Phys. Rev. B*, **2007**, 75, 235106.

[52] S. Ciuchi, S. Fratini. *Phys. Rev. B*, **2012**, 86, 245201.

[53] N. Kirova, M.-N. Bussac. *Phys. Rev. B*, **2003**, 68, 235312.

[54] I. N. Hulea, S. Fratini, H. Xie, C. L. Mulder, N. N. Iossad, G. Rastelli, S. Ciuchi, A. F. Morpurgo, *Nat. Mater.*, **2006**, 5, 982.

[55] T. Richards, M. Bird, H. Sirringhaus, *J. of Chem. Phys.*, **2008**, 128, 234905.

[56] D. A. da Silva Filho, E.-G. Kim, J.-L. Bredas, *Adv. Mater.*, **2005**, 17, 1072.

[57] A. Troisi, *Adv. Mater.*, **2007**, 19, 2000.

[58] K. Hannewald, P. A. Bobbert, *Appl. Phys. Lett.*, **2004**, 85, 1535.

[59] K. Hannewald, Stojanović V. M., J. M. T. Schellekens, P. A. Bobbert, G. Kresse, J. Hafner, *Phys. Rev. B*, **2004**, 69, 075211.

[60] T. Kato, K. Yoshizawa, K. Hirao, *J. Chem. Phys.*, **2002**, 116, 3420.

[61] R. S. Sánchez-Carrera, P. Paramonov, G. M. Day, V. Coropceanu, J.-L. Brédas, *J. Am. Chem. Soc.*, **2010**, 132, 14437.

[62] S. Fratini, S. Ciuchi. *Phys. Rev. Lett.*, **2009**, 103, 266601.

[63] A. J. Heeger, S. Kivelson, J. R. Schrieffer, W. P. Su, *Rev. Mod. Phys.*, **1988**, 60, 781.

[64] M. Capone, W. Stephan, M. Grilli, *Phys. Rev. B*, **1997**, 56, 4484.

[65] M. Zoli, *Phys. Rev. B*, **2002**, 66, 012303.

[66] Y. Okada, K. Sakai, T. Uemura, Y. Nakazawa, J. Takeya, *Phys. Rev. B*, **2011**, 84, 245308.

[67] V. Podzorov, E. Menard, A. Borissov, V. Kiryukhin, J.A. Rogers, M.E. Gershenson, *Phys. Rev. Lett.*, **2004**, 93, 086602.

[68] W. Xie, K. A. McGarry, F. Liu, Y. Wu, P. P. Ruden, C. J. Douglas, C. D. Frisbie, *J. Phys. Chem. C*, **2013**, 117, 11522.

[69] G. D. Mahan, *Many-Particle Physics.* Kluwer Academic/Plenum Publisher, New Yok, **2000**.

[70] S. Fratini, S. Ciuchi, D. Mayou, *Phys. Rev. B*, **2014**, 89, 235201.

[71] Y. C. Cheng, R. J. Silbey, D. A. da Silva Filho, J. P. Calbert, J. Cornil, J. L. Brédas, *J. Chem. Phys.*, **2003**, 118, 3764.

[72] A. J. Millis, J. Hu, S. Das Sarma, *Phys. Rev. Lett.*, **1999**, 82, 2354.

[73] a) O. Gunnarsson, J. E. Han, *Nature*, **2000**, 405, 1027; b) O. Gunnarsson, M. Calandra, J. E. Han, *Rev. Mod. Phys.*, **2003**, 75, 1085.

[74] H. Sumi, *J. Chem. Phys.*, **1979**, 70, 3775.

[75] R. Kubo, *J. Phys. Soc. Japan.*, **1957**, 12, 570.

[76] A. Troisi, *J. Chem. Phys.*, **2011**, 134, 034702.

[77] I.G. Austin, N.F. Mott, *Adv. Phys.*, **1969**, 18, 41.

[78] R. W. Munn, R. Silbey, *J. Chem. Phys.*, **1985**, 83, 1843.

[79] V. M. Kenkre, J. D. Andersen, D. H. Dunlap, C. B. Duke, *Phys. Rev. Lett.*, **1989**, 62, 1165.

[80] F. Ortmann, K. Hannewald, F. Bechstedt, *Appl. Phys. Lett.*, **2008**, 93, 222105.

[81] F. Ortmann, F. Bechstedt, K. Hannewald, *Phys. Rev. B*, **2009**, 79, 235206.

[82] I. G. Lang, Yu. A. Firsov. *Zh. Eksp. Teor. Fiz.*, **1962**, 43, 1843.

[83] I. G. Lang, Yu. A. Firsov. *Sov. Phys. JETP*, **1963**, 16, 1301.

[84] K. Hannewald, V. M. Stojanovć, P. A. Bobbert, *J. Phys.-Condens. Mat.*, **2004**, 16, 2023.

[85] J. Ranninger, *Phys. Rev. B*, **1993**, 48, 13166.

[86] A. S. Alexandrov, P. E. Kornilovitch, *Phys. Rev. Lett.*, **1999**, 82, 807.

[87] M. Berciu, *Phys. Rev. Lett.*, **2006**, 97, 036402.

[88] R. C. Hatch, D. L. Huber, H.t Höchst, *Phys. Rev. Lett.*, **2010**, 104, 047601.

[89] M. Masino, A. Girlando, A. Brillante, L. Farina, R. G. Della Valle, E. Venuti, *Macromol. Sy.*, **2004**, 212, 375.

[90] Y. Li, V. Coropceanu, J.-L. Brédas, *J. of Phys. Chem. Lett.*, **2012**, 3, 3325.

[91] Y. Li, Y. Yi, V. Coropceanu, J.-L. Brédas, *Phys. Rev. B*, **2012**, 85, 245201.

[92] S. Ciuchi, S. Fratini, D. Mayou, *Phys. Rev. B*, **2011**, 83, 081202.

[93] E. Mozafari, S. Stafstrom, *J. Chem. Phys.*, **2013**, 138, 184104.

[94] G. De Filippis, V. Cataudella, S. Fratini, S. Ciuchi, *Phys. Rev. B*, **2010**, 82, 205306.

[95] L. Wang, Q. Li, Z. Shuai, L. Chen, Q. Shi, *Phys. Chem. Chem. Phys.*, **2010**, 12, 3309.

[96] L. Wang, D. Beljonne, L. Chen, Q. Shi, *J. Chem. Phys.*, **2011**, 134, 244116.

[97] H. Ishii, K. Honma, N. Kobayashi, K. Hirose, *Phys. Rev. B*, **2012**, 85, 245206.

[98] H. Tamura, M. Tsukada, H. Ishii, N. Kobayashi, K. Hirose, *Phys. Rev. B*, **2012**, 86, 035208.

[99] H. Ishii, N. Kobayashi, K. Hirose, *Phys. Rev. B*, **2013**, 88, 205208.

[100] H. Ishii, H. Tamura, M. Tsukada, N. Kobayashi, K. Hirose, *Phys. Rev. B*, **2014**, 90, 155458.

[101] P. V. Parandekar, J. C. Tully, *J. Chem. Phys.*, **2005**, 122, 094102.

[102] G. De Filippis, V. Cataudella, S. Mishchenko, A. N. Nagaosa, A. Fierro, A. de Candia, *Phys. Rev. Lett.*, **2015**, 114, 086601.

[103] Y. Yao, W. Si, X. Hou, C.-Q. Wu, *J. Chem. Phys.*, **2012**, 136, 234106.

[104] D. Mayou, *Phys. Rev. Lett.*, **2000**, 85, 1290.

[105] a) G. Trambly de Laissardière, J.-P. Julien, D. Mayou, *Phys. Rev. Lett.*, **2006**, 97, 026601; b) D. Nguyen-Manh, D. Mayou, G. J. Morgan, A. Pasturel, *J. Phys. F: Met. Phys.* **1987**, 17, 999; c) E. Belin, D. Mayou, *Phys. Scripta* **1993**, T49, 356.

[106] J. M. Moix, M. Khasin, J. Cao, *New J. Phys.* **2013**, 15, 085010.

[107] D. M. Packwood, K. Oniwa, T. Jin, N. Asao, *J. Chem. Phys.* **2015**, 142, 144503.

[108] M. Dressel, G. Grner, *Electrodynamics of Solids - Optical Properties of Electron in Matter.* Cambridge University Press, 2002.

[109] D. J. Thouless, *Phys. Rev. Lett.*, **1977**, 39, 1167.

[110] a) G. Trambly de Laissardière, Didier Mayou, *Phys. Rev. Lett.*, **2013**, 111, 146601; b) P. Darancet, V. Olevano, D. Mayou. *Phys. Rev. B* **2010**, 81, 155422; c) S. Roche, D. Mayou, *Phys. Rev. B* **1999**, 60, 322; d) D. Mayou, S. Khanna, *J. Phys. I*, **1995**, 5, 1199; e) D. Mayou *Europhys. Lett.* **1988**, 6, 549.

[111] H. Dong, X. Fu, J. Liu, Z. Wang, W. Hu, *Adv. Mater.*, **2013**, 25, 6158.

[112] Y. Yuan, G. Giri, A. L. Ayzner, A. P. Zoombelt, S. C. B. Mannsfeld, J. Chen, D. Nordlund, M. F. Toney, J. Huang, Z, Bao, *Nat. Commun.*, **2014**, 5, 3005.

[113] K. A. McGarry, W. Xie, C. Sutton, C. Risko, Y. Wu, V. G. Young, J.-L. Brédas, C. D. Frisbie, C. J. Douglas, *Chem. Mater.*, **2013**, 25, 2254.

[114] J. C. Tully, *J. Chem. Phys.*, **1990**, 93, 1061.

[115] A. V. Akimov, R. Long, O. V. Prezhdo, *J. Chem. Phys.*, **2014**, 140, 194107.

[116] V. Cataudella, G. De Filippis, C. A. Perroni, *Phys. Rev. B*, **2011**, 83, 165203.

[117] N. V. Prokof'ev, B. V. Svistunov, *Phys. Rev. Lett.*, **1998**, 81, 2514.

[118] M. Jarrell, J.E. Gubernatis, *Phys. Rep.*, **1996**, 269, 133.

[119] D. J. J. Marchand, G. De Filippis, V. Cataudella, M. Berciu, N. Nagaosa, N. V. Prokof'ev, A. S. Mishchenko, P. C. E. Stamp, *Phys. Rev. Lett.*, **2010**, 105,266605.

[120] R. Uchida, H. Yada, M. Makino, Y. Matsui, K. Miwa, T. Uemura, J. Takeya, H. Okamoto, *Appl. Phys. Lett.*, **2013**, 102, 093301.

[121] V. I. Mel'nikov, A. A. Gogolin, E. I. Rashba, *Sov. Phys. JETP*, **1975**, 42, 168.

[122] E.I. Rashba, A.A. Gogolin, V.I. Mel'nikov, In *Organic Conductors and Semiconductors*, volume 65 of *Lecture Notes in Physics*, (Eds. L. Pal, G. Gruner, A. Janossy, and J. Solyom), Springer Berlin Heidelberg, **1977**, pp. 265–280.

[123] M. Jonson, S. M. Girvin. *Phys. Rev. Lett.*, **1979**, 43, 1447.

[124] A. Madhukar, M. H. Cohen, *Phys. Rev. Lett.*, **1977**, 38, 85.

[125] A. A. Gogolin, V. I. Mel'nikov, E. I. Rashba, *Sov. Phys. JETP*, **1977**, 45, 330.

[126] a) A.A. Gogolin, *Phys. Rep.*, **1982**, 86, 1; b) A.A. Gogolin, *Phys. Rep.*, **1988**, 166, 269.

[127] A.A. Gogolin, G.T. Zimanyi, *Solid State Commun.*, **1983**, 46, 469.

[128] A.A. Gogolin, G.T. Zimanyi, *Solid State Commun.*, **1984**, 50, 791.

[129] V. K. S. Shante, *J. Phys. C: Solid State Physics*, **1978**, 11, 2561.

[130] K. Takenaka, M. Tamura, N. Tajima, H. Takagi, J. Nohara, S. Sugai, *Phys. Rev. Lett.*, **2005**, 95, 227801.

[131] K. Hashimoto, S. C. Zhan, R. Kobayashi, S. Iguchi, N. Yoneyama, T. Moriwaki, Y. Ikemoto, T. Sasaki, *Phys. Rev. B*, **2014**, 89, 085107.

[132] S. Mahmoudian, L. Rademaker, A. Ralko, S. Fratini, V. Dobrosavljević, preprint arXiv:1412.4441.

[133] H. Seo, J. Merino, H. Yoshioka, M. Ogata, *J. Phys. Soc. Jpn.*, **2006**, 75, 051009.

[134] L. Cano-Cortés, J. Merino, S. Fratini, *Phys. Rev. Lett.*, **2010**, 105, 036405.

[135] A. Graja, *Low-Dimensional Organic Conductors*, World Scientific, **1992**.

[136] M. Dressel, N. Drichko, *Chem. Rev.* , **2004**, 104, 5689.

[137] W. Xie, S. Wang, X. Zhang, C. Leighton, C. D. Frisbie, *Phys. Rev. Lett.*, **2014**, 113, 246602.

[138] T. Kampfrath, K. von Volkmann, C. M. Aguirre, P. Desjardins, R. Martel, M. Krenz, C. Frischkorn, M. Wolf, L. Perfetti, *Phys. Rev. Lett.*, **2008**, 101, 267403.

[139] M. Ichida, S. Saito, T. Nakano, Y. Feng, Y. Miyata, K. Yanagi, H. Kataura, H. Ando, *Solid State Commun.*, **2011**, 151, 1696.

[140] R. Ulbricht, E. Hendry, J. Shan, T. F. Heinz, M. Bonn, *Rev. Mod. Phys.*, **2011**, 83, 543.

[141] G. S. Engel, T. R. Calhoun, E. L. Read, T.-K. Ahn, T. Mancal, Y.-C. Cheng, R. E. Blankenship, G. R. Fleming, *Nature*, **2007**, 446, 782.

[142] M. Mohseni, P. Rebentrost, S. Lloyd, A. Aspuru-Guzik, *J. Chem. Phys.*, **2008**, 129, 174106.

[143] P. Rebentrost, M. Mohseni, I. Kassal, S. Lloyd, A. Aspuru-Guzik, *New J. Phys.*, **2009**, 11, 033003.